Saltwater Intrusion Vulnerability Assessment in Plymouth, MA - Compounding Effects of Sea Level Rise on Water Quality and Aquifer Sustainability

By the University of Massachusetts Amherst Hydrogeology Group

Alexander Kirshen, Carly Lombardo, David Boutt, Daniel Corkran, Brendan Moran, & Rachel King

October 2023

Table of Contents

Executive Summary

With climate change and rising sea levels, coastal communities that rely on groundwater are at increasing risk of saltwater intrusion which could cause salinity increases in coastal water bodies and drinking water. Salinity increases can degrade soils, drinking water, biodiversity, human health, and infrastructure. In this report, we present the results of our 2-year study investigating both the current status of saltwater intrusion and future saltwater intrusion through the year 2100 into the Plymouth, Massachusetts coastal aquifer. We created a salinity database with groundwater and surface water samples and mapped modern salinity distributions. We then developed a groundwater flow and transport model based on the existing USGS groundwater flow model for the region to assess how future changes in sea level, groundwater pumping, and groundwater recharge will impact the location of the freshwater-saltwater interface and the salinity of wells and ponds. These future climate and pumping scenarios were generated with the latest sea level rise and water use projections.

Based on our results, the current (2023) state of saltwater intrusion shows localized increases in subsurface salinity (saltwater) in the aquifer along the coast. At the aquifer scale, specific land uses including road salt and septic return flows are the dominant sources of salinity to the aquifer. The forward-looking model simulations predict the freshwater-saltwater interface will migrate 100 to 500 meters inland and aquifer salinities will increase by 0 to 17,000 mg/L by 2100 due to sea level rise and pumping. Based on simulated pond concentrations, Allens Pond, Scokes Pond, and Center Hill Pond are most at risk of saltwater intrusion; these ponds are at low elevations (1 to 3 m) and close to the coast (less than 150 m). Model simulations identify one pumping well to be at risk of future elevated salinity concentrations: DEP Well 4036002-02G.

Variations in pond and well salinities from a sensitivity analysis show that septic system re-infiltration buffers saltwater intrusion. We also find that terrestrial recharge plays an important role in limiting saltwater intrusion; compared to simulations with modern recharge rates, the mixing zone was predicted to migrate 100 to 700 meters further inland by 2100 with a 15% reduction in recharge. Based on the modeling results presented we have the following recommendations and suggestions:

- Develop and maintain a salinity database for surface and groundwaters across the town and create a public dashboard for open access to salinity observations in town water supply wells.
- Raise funds to perform an airborne electromagnetic geophysical survey of coastal areas to image the extent of saltwater intrusion to validate modeling projections and document the hydrostratigraphic architecture of key coastal areas (See 'Hydrostratigraphy and Geophysical Survey' section).
- Develop an early warning system for subsurface salinity changes in key coastal areas (See 'Early Warning System and Optimal Well Placement' section).
- Consider the suggested recommendations in the 'Early Warning System and Optimal Well Placement' section for optimal placement of freshwater production wells.

Introduction

With climate change and rising sea levels, coastal communities that rely on groundwater are at increasing risk of saltwater intrusion. By 2100, sea level in Boston, Massachusetts is projected to rise 43.0 to 180.5 cm from 2020 levels. Rising sea levels can trigger the landward movement of saline water beneath the ocean into fresh groundwater aquifers (saltwater intrusion), which could cause salinity increases in coastal water bodies and drinking water (Douglas & Kirshen, 2022). Saltwater intrusion may also be exacerbated by pumping, land use changes, and climate variations, both through sea level rise and changes in terrestrial groundwater recharge (Bosserelle et al., 2022). However, saltwater intrusion is not the only source of salt to groundwater and surface water systems; other sources include sewage, fertilizer, road salt, and drinking water treatment (Kaushal, et al. 2021). Salinity increases can degrade soils, drinking water, biodiversity, human health, and infrastructure (Kaushal, et al. 2021).

The coastal area of Plymouth, Massachusetts is underlain by a dynamic freshwater-saltwater interface (or transition zone) (Figure 1). The location and geometry of the freshwater-saltwater interface can shift over time causing salinity changes in drinking wells, ponds, and groundwater. For this study, we created a salinity database for Plymouth with chloride (Cl^-), specific conductance (SC), and total dissolved solids (TDS) data from surface water (streams and ponds) and groundwater. We mapped TDS concentrations to understand current salinity distributions and potential causes of elevated concentrations. We then developed a groundwater flow and transport model to assess how future changes in sea level, groundwater pumping, and groundwater recharge will impact the location of the freshwater-saltwater interface and the salinity of wells and ponds.

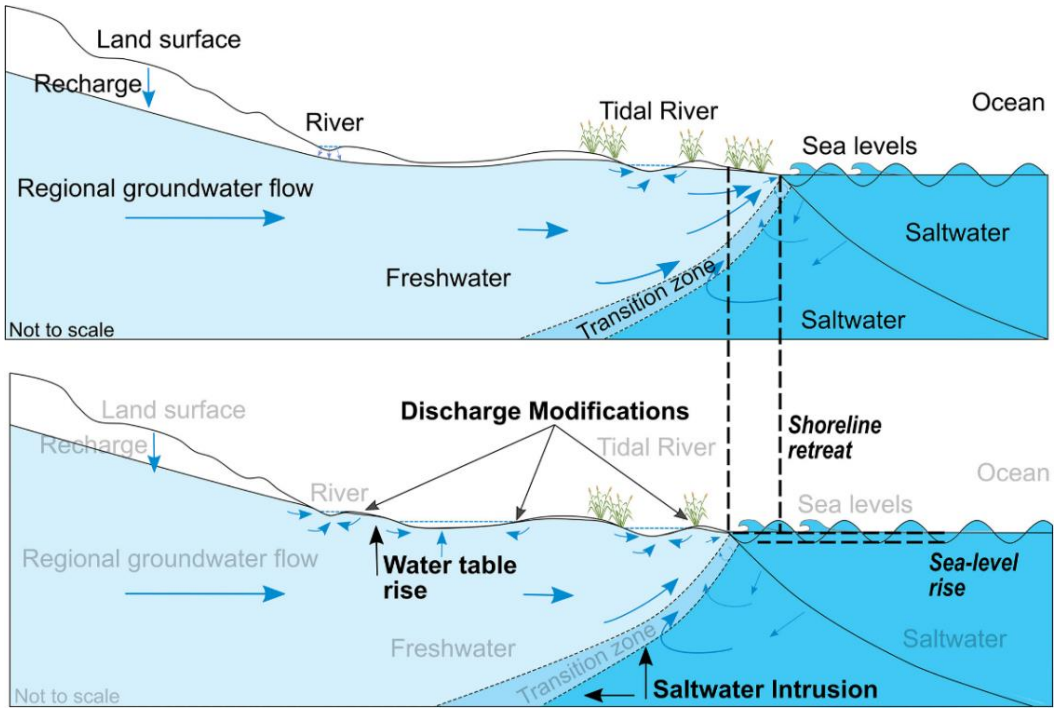

Figure 1: Schematic from Bosserelle et al. (2022) showing how sea level rise can cause saltwater intrusion and increases in water table elevations.

Salinity Database and Mapping

Data and Methods

To examine salinity distributions in and around Plymouth, we created a salinity database. The database contains all available data from groundwater wells and surface water from the area. We extracted the data from several sources including the USGS Nation Water Information System (NWIS), Massachusetts Department of Environmental Protection (MassDEP) Drinking Water Quality Data, UMass Acid Rain Monitoring Program, Cape Cod Rivers Observatory, and Tidmarsh Living Observatory. The age range for the extracted water samples is from 1980 to 2022. In addition to extracting salinity data from public domain websites, we also performed our own salinity analysis by measuring the chloride content in groundwater well samples that were provided by local residents of the Plymouth area.

The data were organized into three categories: 1) public water supply wells (PWS), 2) non-PWS groundwater wells, and 3) surface water. Some samples did not include all three measurements (Cl^-, SC, and TDS), in which case we converted the available data to estimate the missing parameter using standard relationships between Cl^-, SC, and TDS. The conversion factors were calculated from samples that were measured for all three parameters, and these conversions are within the range of previous studies (Rusydi, 2018; Hem, 1985). To map TDS distributions, mean TDS values were calculated for each sample site within a 5-mile buffer of the groundwater model domain and interpolated using natural neighbor. We then compared the results to the Environmental Protection Agency (EPA) National Secondary Drinking Water Regulations. The recommended maximum concentrations for chloride and TDS are 250 mg/L and 500 mg/L, respectively.

Results

The average total dissolved solids concentrations in PWS wells range from 25 to 419 mg/L, with the highest value in Carver (Figure 2). Hotspots with TDS values reaching ~300 to 400 mg/L are in Hanover, Plympton, Cedarville, and Carver. These hotspots are in locations with industrial facilities, businesses, schools, and housing developments. For the PWS wells located in towns along the coast, TDS values are between ~100 to 300 mg/L. PWS wells in areas with the least development, like Myles Standish State Forest, have low TDS (less than 100 mg/L). All TDS values from PWS wells fall within the EPA's safe drinking water recommendation.

When considering all groundwater samples (PWS and Non-PWS), average TDS concentrations range from 3 to 640 mg/L (Figure 3). The highest average value is the Town of Plymouth well 500 meters north of Russel Mill Pond, just west of Rt. 3; this well is also within 1 km of the Plymouth Sewer Department and other developments. Due to the proximity of the highway and these developments, road salt could be the main cause of elevated TDS in this well. The other town wells (14 in total) have TDS values less than 230 mg/L. The other well with TDS over 500 mg/L (630 mg/L) is in Hanover in the northwest of the study area; this well is in a residential area near industrial facilities. Similar to the PWS data, urbanized areas have higher concentrations than less developed regions (campgrounds and forests). Kingston, Duxbury, and Cedarville, which all lie near the coast, have TDS ranges of ~200 to 300 mg/L. The vast majority (99%) of sites fall within the EPA's safe drinking water recommendation.

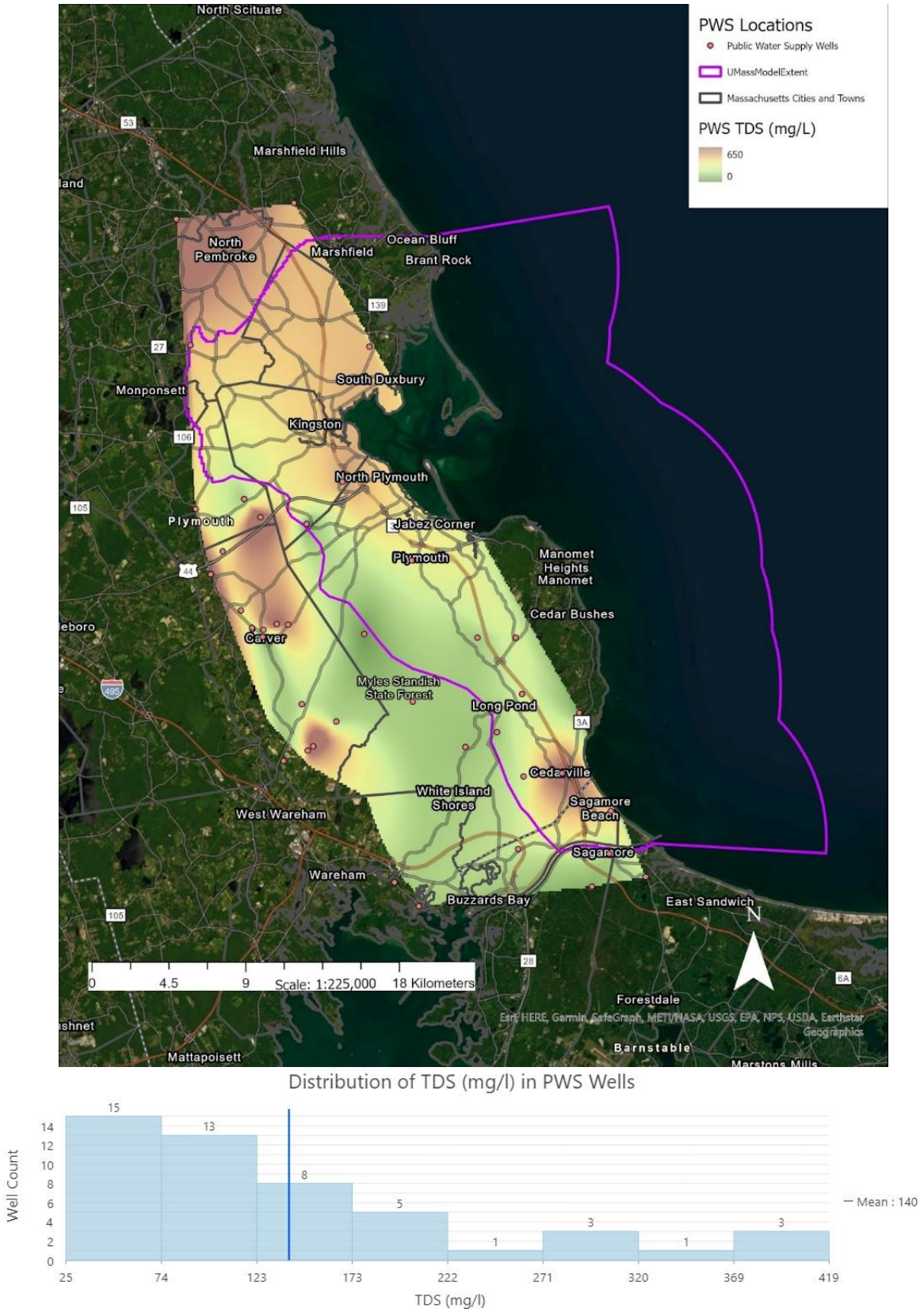

Figure 2: Average total dissolved solids (TDS) for all public water supply (PWS) wells interpolated using natural neighbor. Below is a histogram of results with the blue line representing the mean.

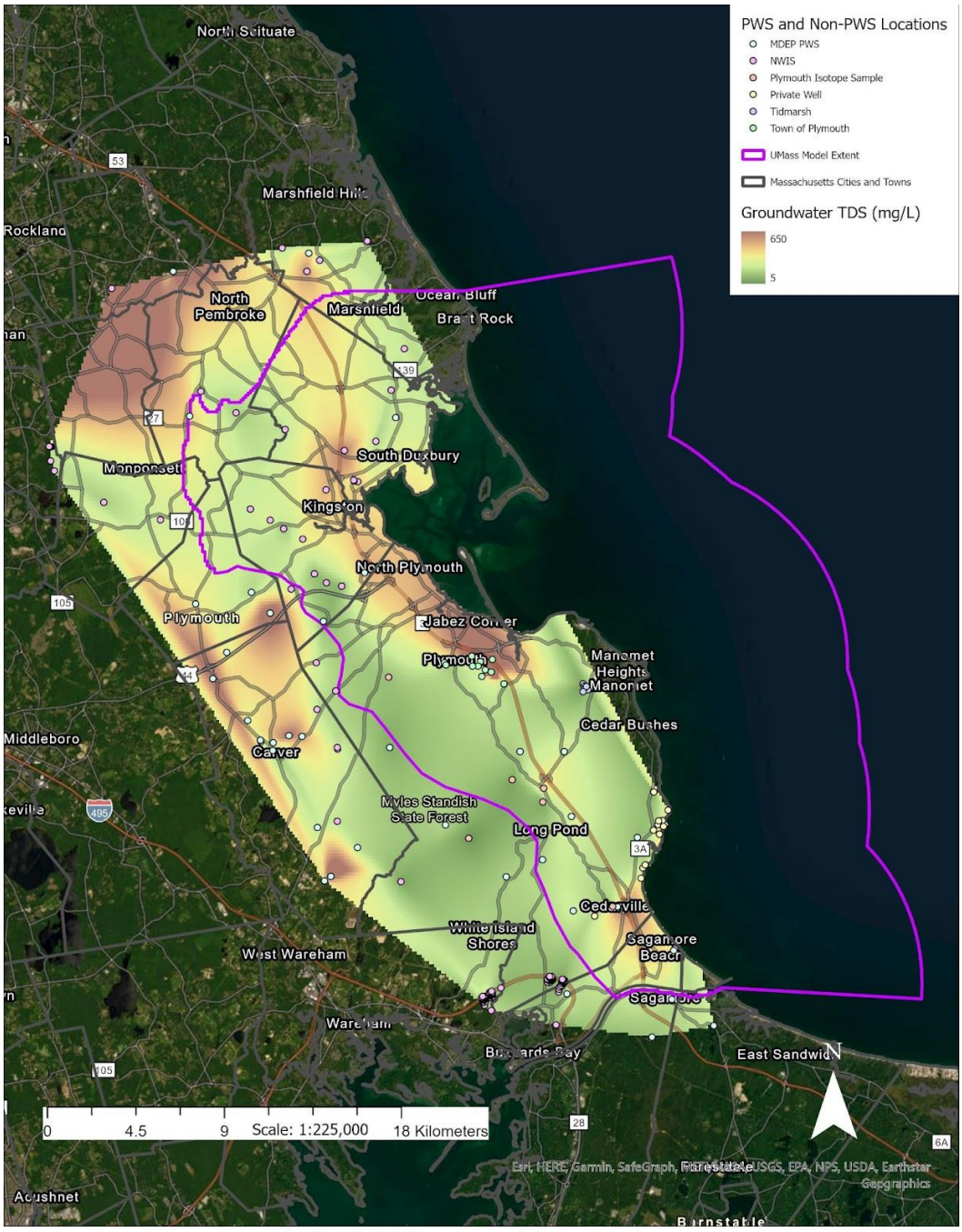

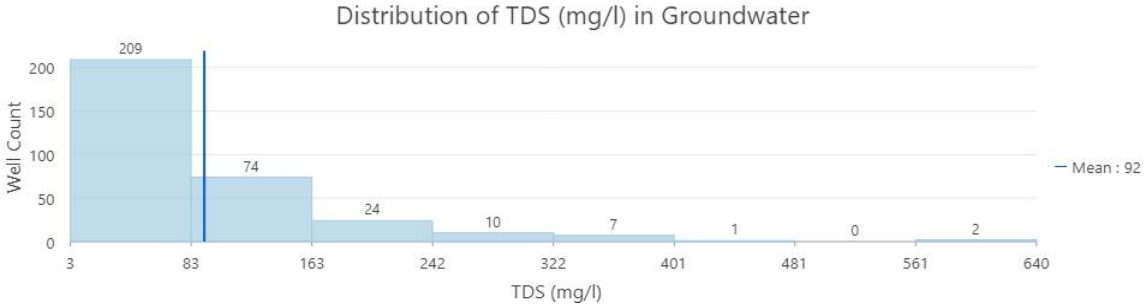

Figure 3: Average total dissolved solids (TDS) for all groundwater data interpolated using natural neighbor. Below is a histogram of results with the blue line representing the mean.

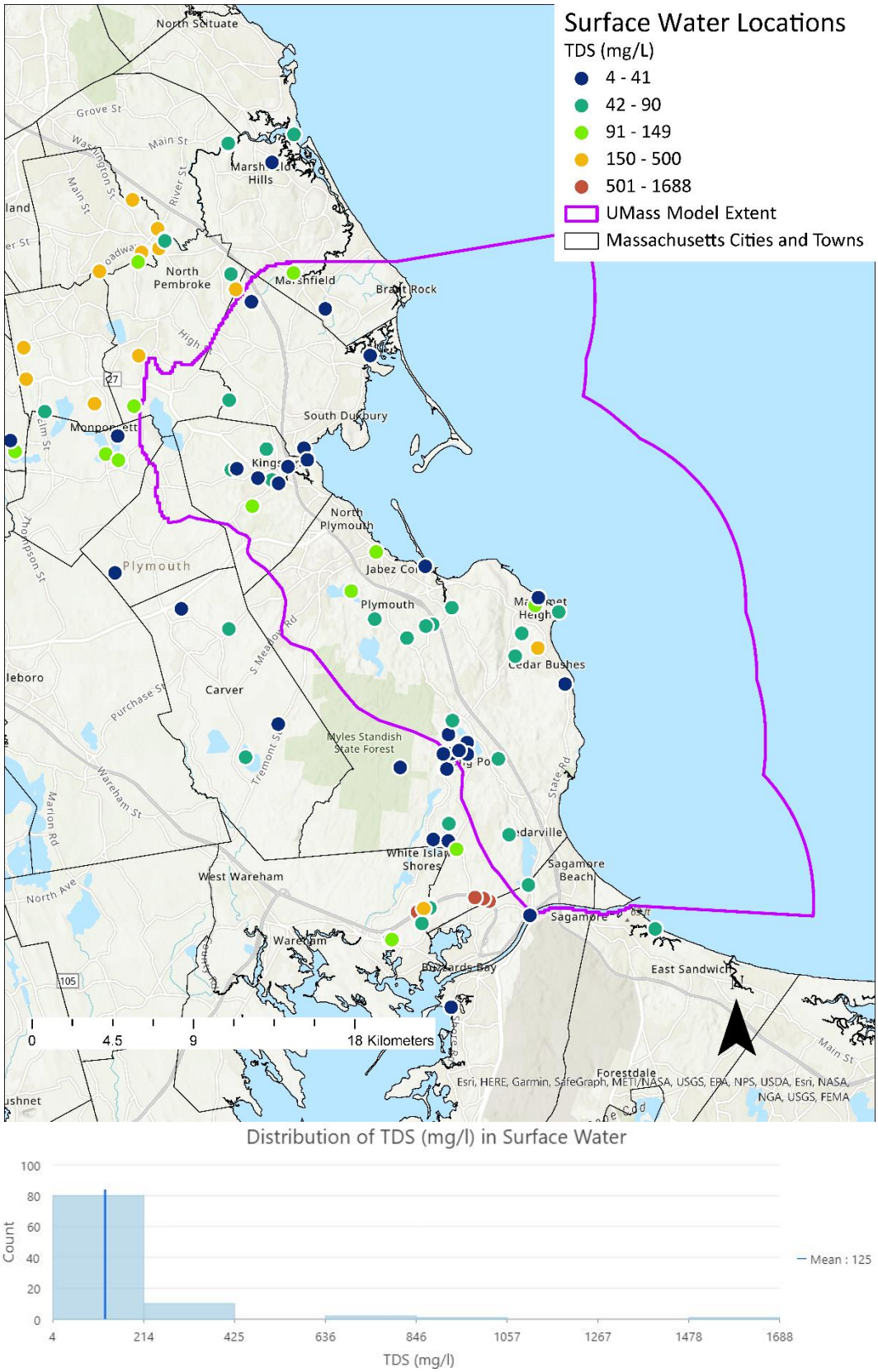

Figure 4: Average total dissolved solids (TDS) for all surface water samples. Below is a histogram of results with the blue line representing the mean.

Average surface water TDS values have a range of 4 to 1688 mg/L (Figure 4). The four sites that have average TDS concentrations greater than 500 mg/L are between the Cape Cod Canal and the White Island Shores area near the southwest of the model domain; these sites are along Rt. 25, so the likely cause of these elevated concentrations is road salting. Other hotspots are located in the North Pembroke - Hanover region with average TDS values ranging from ~150 to 350 mg/L and near Manomet (average TDS of 257 mg/L). All other sampled surface water locations within the Plymouth area have relatively low concentrations.

We observe that elevated TDS concentrations in surface water and groundwater occur primarily in urbanized settings and that sample locations near the ocean do not generally exhibit elevated TDS concentrations. Therefore, the likely causes of historical elevated TDS concentrations in groundwater and surface water are related to human activities, not sea level rise or saltwater intrusion. With cold snowy winters and below-freezing temperatures common in this region, road salt is regularly applied to prevent ice from forming on roads. Relatively high TDS values near major highways are likely due to the towns salting their roads during the winter months. Other relatively high groundwater concentrations are located near places with typically high human activity, such as businesses, schools, and housing developments. To better understand the contribution of road salt to elevated salinities, a future study could analyze seasonal TDS variations near major roads and highways.

Groundwater Flow and Transport Model

Model Domain, Boundary Conditions, and Calibration

We developed a numerical variable-density groundwater flow model of the Plymouth, Carver, Kingston, Duxbury (PCKD) aquifer using the groundwater modeling software MODFLOW 6 (Langevin et al., 2023). The 595 km^2 model domain was modified from Masterson et al. (2009) and contains portions of Marshfield, Pembroke, Duxbury, Kingston, Plympton, Plymouth, and Borne. The western boundary represents a groundwater divide delineated from the steady-state head distribution from Masterson et al. (2009), and the eastern boundary extends ~5 km offshore (Figure 5 and Figure 6). The top of the model domain represents the ground surface and was developed by merging the MassGIS 1 meter Lidar DEM with the Massachusetts Coastal Zone Bathymetry from Andrews et al. (2018). The bottom of the model domain represents 15 m below the top of bedrock. We identified the bedrock surface by merging the bedrock elevation map from Mabee et al. (2022) and a modified version of the offshore bedrock elevation from Stone & Stone (2019). The model contains 18 layers with model cells 100 m wide and 100 m long. Cell thickness varies based on ground surface elevation and proximity to sea level. Cell thicknesses are 4 m from elevations 8 to -32 m, 8 m thick from elevations -32 to -56 m, and 16 m thick from elevations -56 to -120 m. The top elevation of cells representing the ground surface was set to the top of ground surface mentioned above and ranged in thickness from 0.1 to 116 m. All mentioned elevations in this report are referenced to the North American Vertical Datum of 1988 (NAVD 88).

Boundary conditions are assigned to the model to represent environmental and anthropogenic forcings. The model represents the effects of sea level using a specified-head (Dirichlet) boundary using the constant head (CHD) package. The constant head (CHD) boundary is assigned to cells with cell top elevations less than 0 m along the top of the active model domain. Baseline sea level for the CHD boundary is the mean hourly sea level from April 2022 to April 2023 from the NOAA

Water Levels database at the Boston, MA site (0.052 m NAVD 88). Recharge with a TDS concentration of 100 mg/L enters the top of the model except for in the ocean (CHD cells), which is represented by a specified flux (Neumann) boundary using the recharge (RCH) package. Recharge varies for glacial aquifer sediments (0.0019 m/day), ponds (0.0014 m/day), wetlands (0.0005 m/day), and cranberry bogs (0.0007 m/day) (Masterson et al., 2009). We represent streams and rivers with a head-dependent flux (Robin) boundary using the river (RIV) package. Conductance for the rivers was calculated using a vertical hydraulic conductivity of 6.1 m/day, stream width of 3 m, and variable stream length based on the length of the stream within each cell (Masterson et al., 2009). Ponds, lakes, and reservoirs with an area greater than 8,000 m^2 (186 total) were modeled as high hydraulic conductivity zones with values ranging from 1,332 to 15,240 m/day. Pond hydraulic conductivities were calculated as the ratio of pond depth to cell thickness multiplied by 15,240 m/day (or 50,000 ft/day) (Masterson et al., 2009).

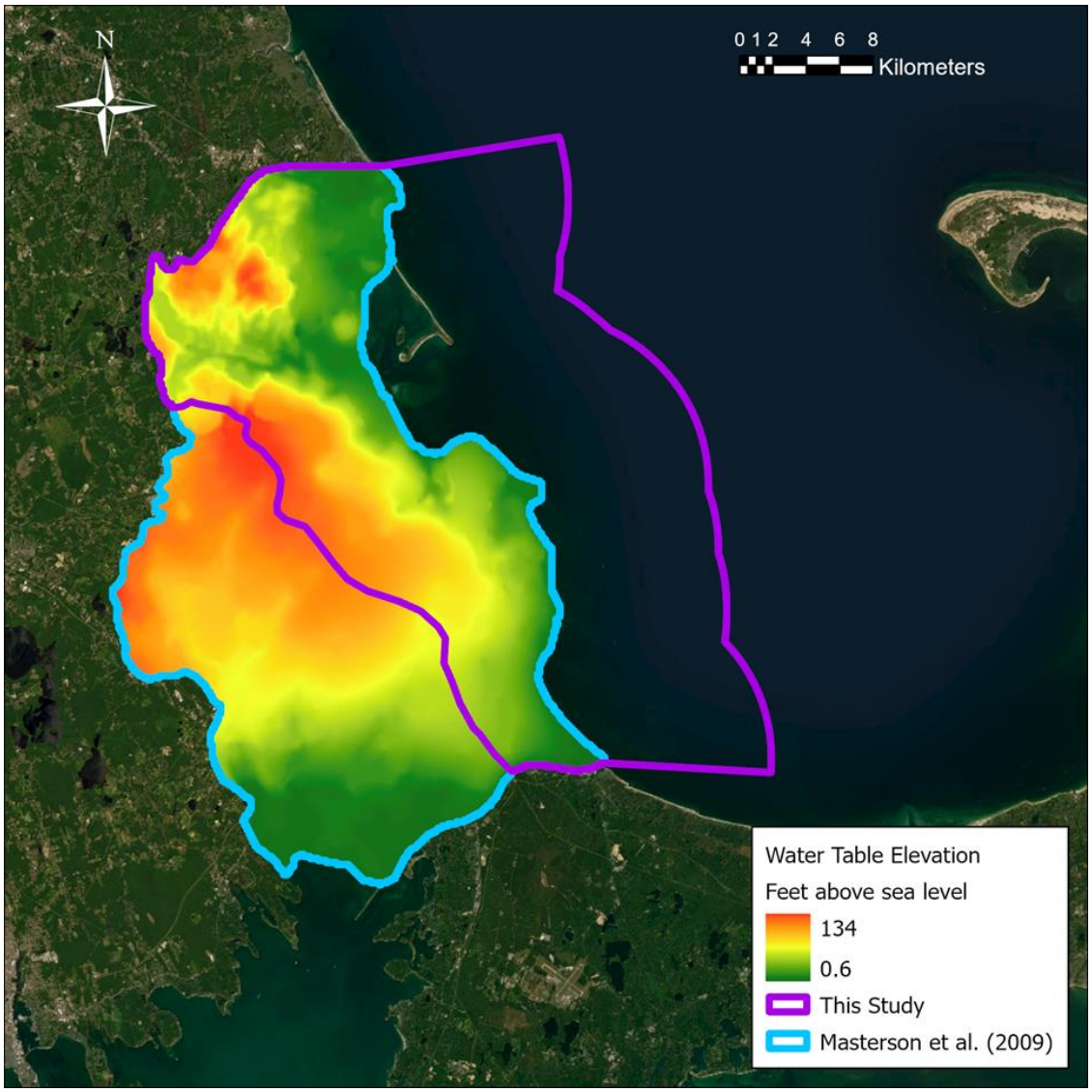

Figure 5: Model domain and steady-state hydraulic head from Masterson et al. (2009) and the modified model domain from this study.

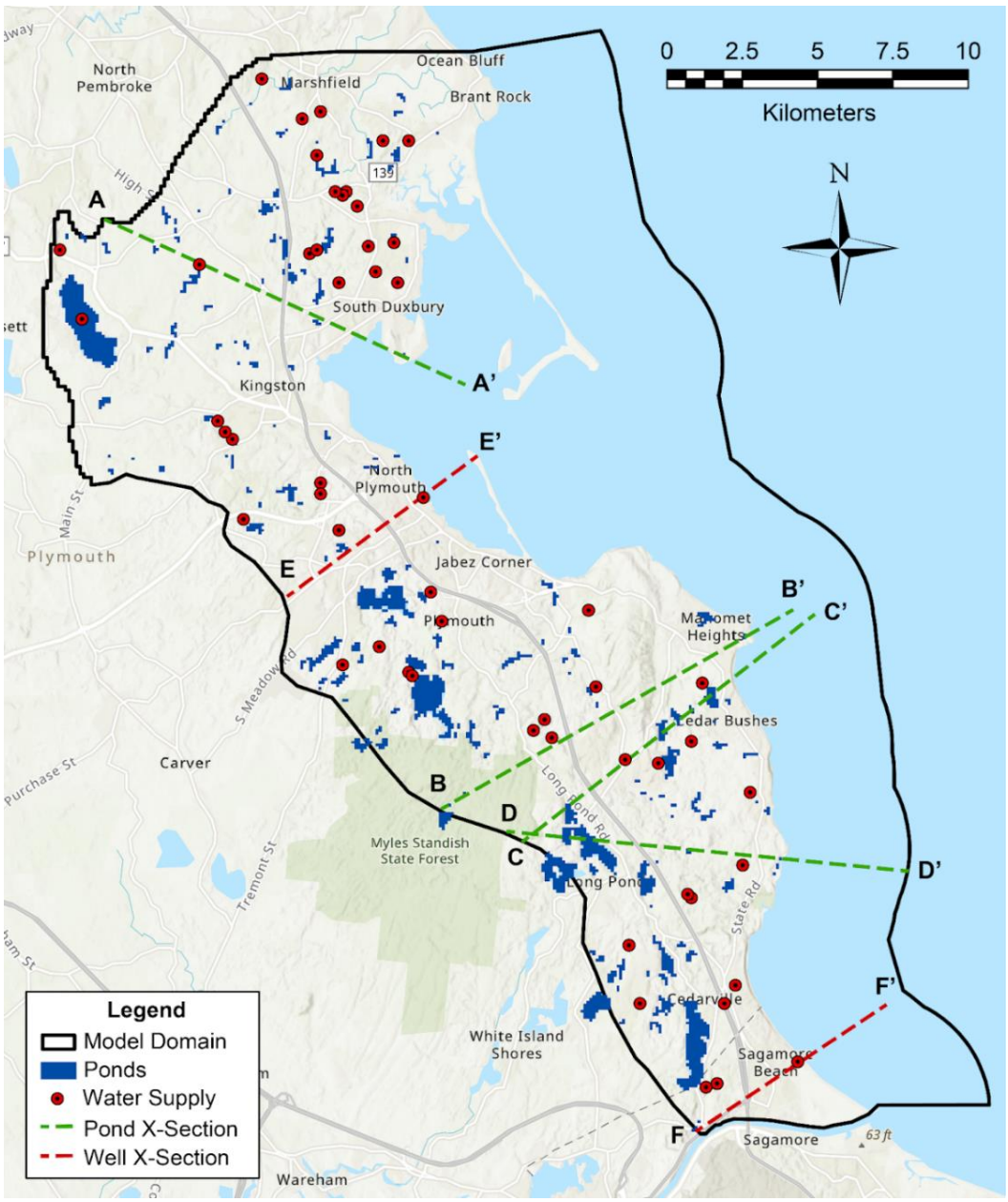

Figure 6: Site map with model domain (black polygon), ponds (blue polygons), modeled water supply (red circles), and locations of cross-section lines from Figures 9 and 16. The cross-sections are approximately parallel to fluid flow.

Anthropogenic forcings consist of pumping wells, centralized wastewater re-infiltration, and septic system return flow. We represent pumping wells and centralized wastewater re-infiltration as a specified flux (Neumann) boundary condition using the well (WEL) package and septic system return flow using the RCH package. Septic system return flow and centralized wastewater re-infiltration have specified TDS concentrations of 100 mg/L. Public water supply wells and centralized wastewater re-infiltration sites are based on the 2030 projections from the Masterson et al. (2009) model, and septic system return flow locations are assigned to cells containing waterlines but no sewer lines (Masterson et al., 2009). Along the eastern margin of the model, a constant

concentration (CNC) boundary with a TDS of 35,000 mg/L represents ocean salinity. For locations of the boundary conditions, see Figure S5 to Figure S11.

Baseline well pumping values were calculated using data from the 2019 Plymouth Draft Water System Master Plan Report. Pumping locations, elevations, and discharge were extracted from the projected 2030 model from Masterson et al. (2009). Total discharge in Plymouth for the year 2023 from the projected water demand forecast in the Draft Report was compared to discharge from the corresponding wells from Masterson et al. (2009). The 2023 Draft Report values comprise 77% of discharge from the 2030 model values. To calculate initial pumping for this model, all 2030 Masterson et al. (2009) production, commercial, and centralized re-infiltration discharge was multiplied by this factor of 0.77. Irrigation well pumping was not changed because irrigation was not predicted to have relevant increases between 2005 and 2030 (Masterson et al., 2009). Septic system return flows were divided into 6 zones based on Masterson et al. (2009) - Plymouth, North Sagamore, Duxbury, Marshfield, Pembroke, and Kingston. We assume that 85% of commercial and production well pumping is re-infiltrated via centralized wastewater return flow (onshore and offshore) and septic system return flow. Starting pumping values for irrigation already account for a 50% re-infiltration rate (Masterson et al., 2009).

The groundwater flow model was calibrated with 36 groundwater and 36 surface water observation points (72 total) from Table 1-6 in the Masterson et al. (2009) report by modifying hydraulic conductivity (Table S1 and Figure 7). To define the extents of hydrogeologic units, we mapped the terrestrial hydrogeologic zones from Masterson et al. (2009) to our model domain (24 total). The

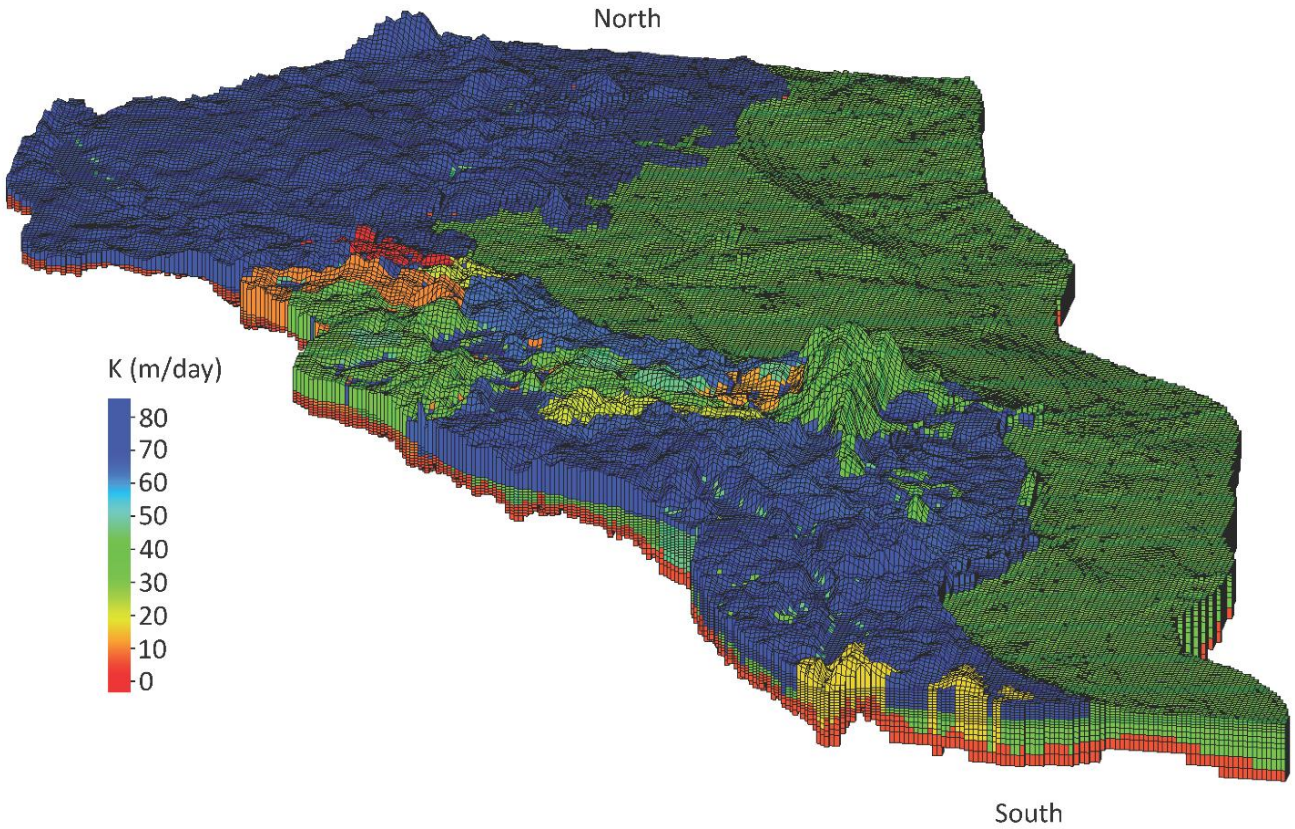

Figure 7: Oblique view of model domain with color representing calibrated hydraulic conductivity (K) in meters per day.

offshore deposits and bedrock aquifer (the volume below the bedrock surface) were defined as two separate hydrogeologic units. The root mean squared error (RMSE) and mean absolute error (MAE) for observed vs. simulated hydraulic heads are 2.0 m (5.5%) and 1.4 m (3.8%), respectively (Figure S1). See Figure S2 for modern hydraulic head distribution.

Modern Salinity Distribution

The calibrated groundwater flow model simulates the modern groundwater flow and salinity distributions for the PCKD aquifer. The modern salinity distribution for the year 2023 falls within TDS ranges of 90 to 35,000 mg/L (Figure 8 and Figure 9). Fresh groundwater and saline

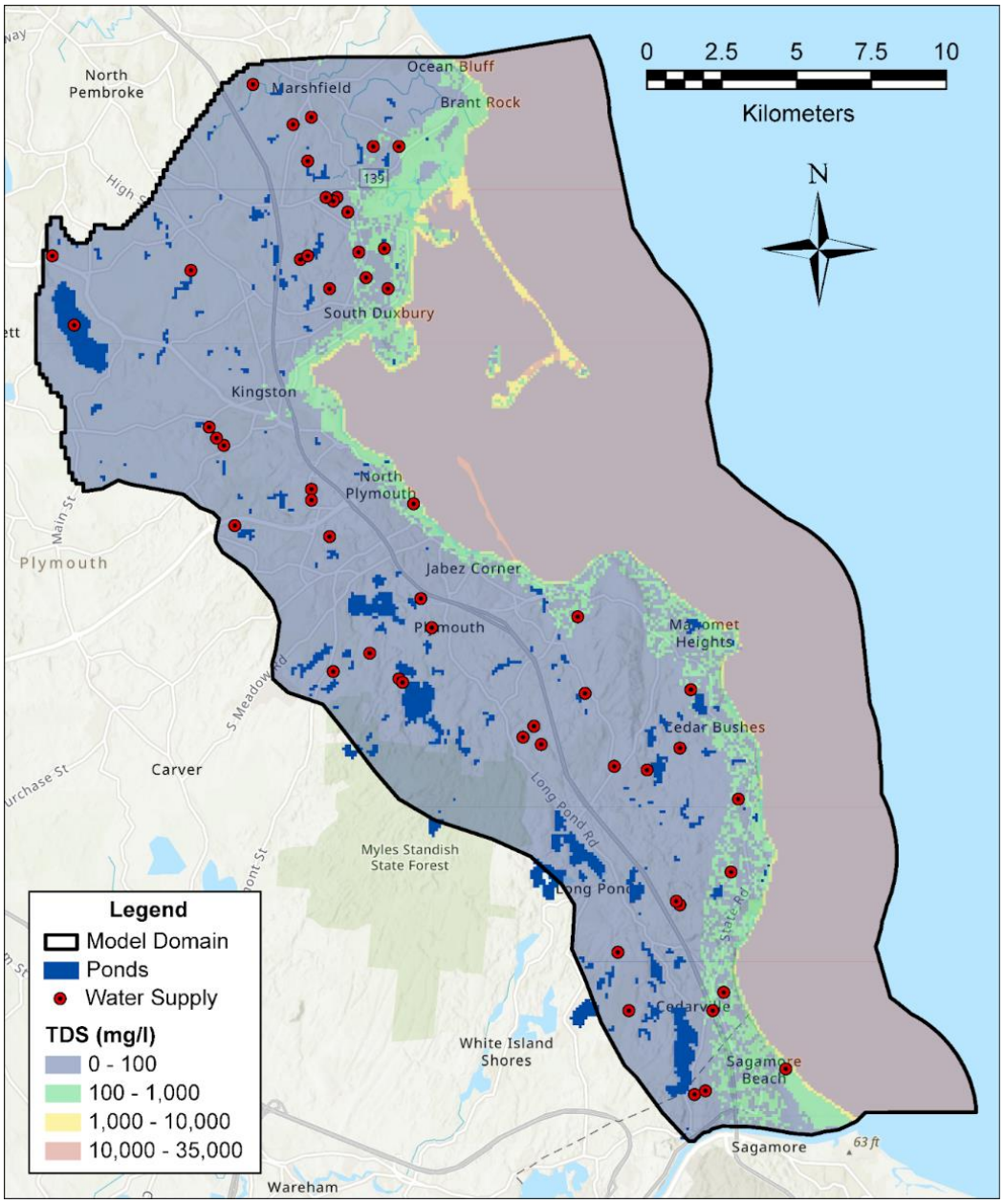

Figure 8: Simulated modern salinity distribution (TDS) in 2023 with locations of modeled water withdrawals and ponds.

groundwater have concentrations of 0-100 mg/L (blue) and 10,000-35,000 mg/L (red), respectively. The freshwater-saltwater mixing zone has concentrations of 1,000-10,000 mg/L (yellow). In general, this zone begins where the land surface meets the ocean and is 100 to 200 meters wide at the water table. Elevated TDS concentrations of 100-1,000 mg/L (green) extend 100 to 4,000 m landward (Figure 8).

Three ponds have TDS concentrations above 100 mg/L: Allens Pond, Scokes Pond, and Center Hill Pond. The relationship between pond geometry and the freshwater-saltwater mixing zone is shown in Figure 9, and the location of these cross-sections is in Figure 6. The mixing zone (1,000-10,000 mg/L) is represented by the light blue and light green colors. The horizontal distance between the mixing zone and Allens Pond, Scokes Pond, and Center Hill Pond are 100, 200, and 0 m, respectively. Only one of these ponds had measured (or observed) TDS; the measured TDS concentration of Scokes Pond was reported as 66 mg/L. Although no measurement of pond salinity was made for Center Hill Pond, there are wells within 50 m of Center Hill Pond that had measured TDS values of up to 316 mg/L.

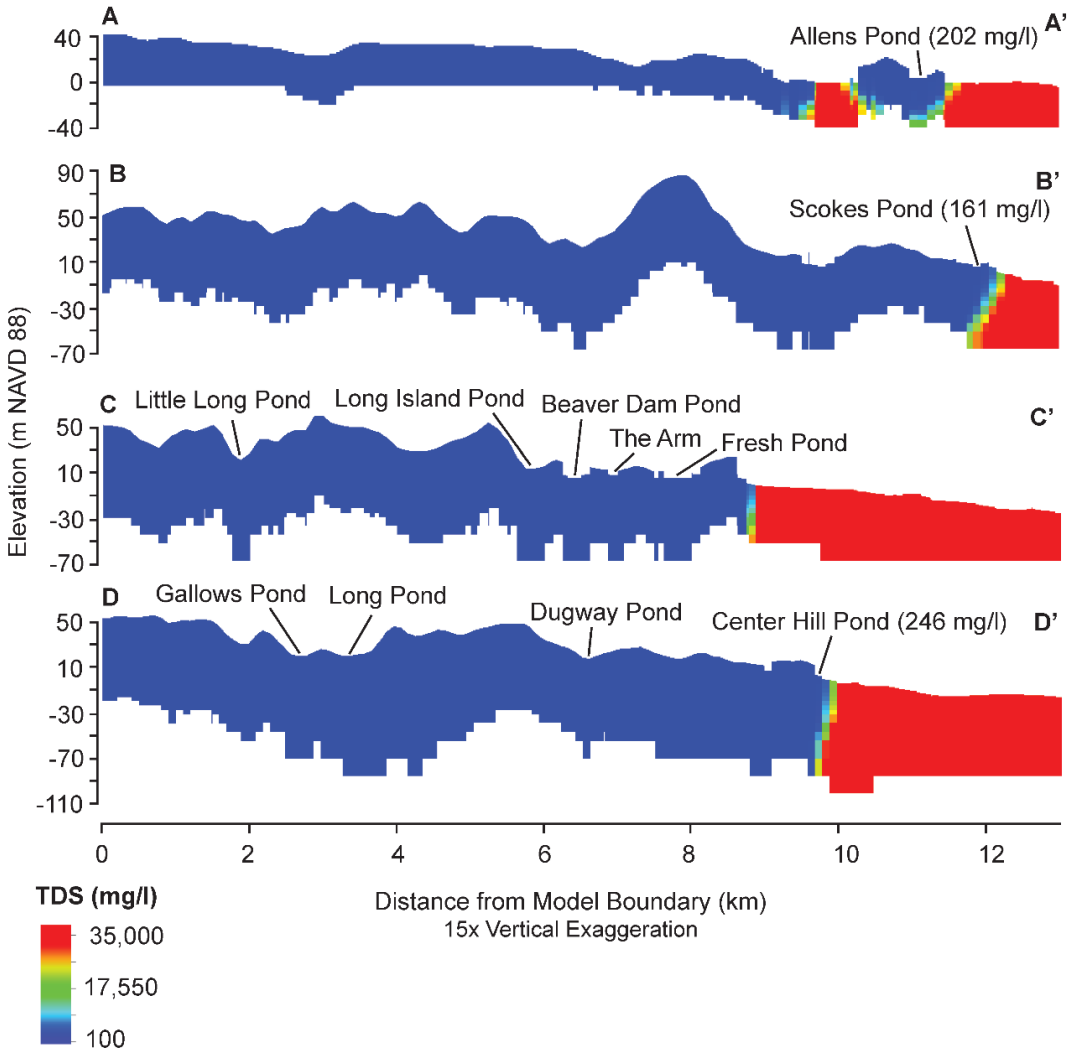

Figure 9: Cross-sections through coastal ponds (labeled) showing the top and bottom model boundaries and modern salinity distributions (color). All ponds have TDS concentrations of 100 mg/L if not otherwise labeled**.** Locations of the cross-sections are shown in Figure 6.

Projected Pumping, Climate Scenarios, and Simulations

We developed a projected pumping scenario through 2100 based on the Draft 2019 Plymouth Master Water Plan Report and an informal discussion with an engineer from Environmental Partners - the consulting group leading the report (Figure 10). It is important to note that the projection beyond 2040 has not been evaluated by an engineer or planner. The Draft Report calculates future water demand in Plymouth through 2040 based on historic water use and projected population growth.

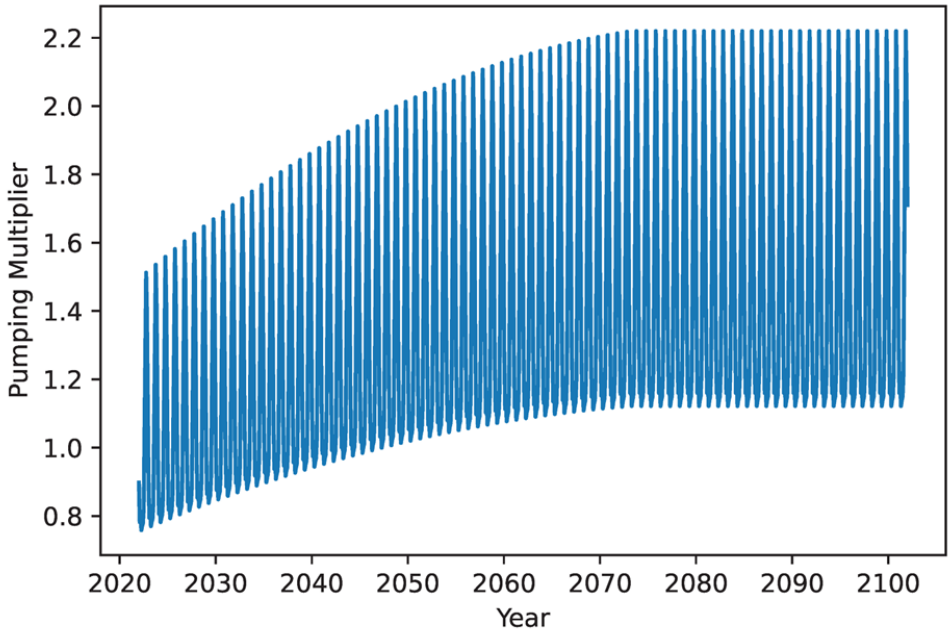

Figure 10: Projected water demand multiplier applied to all commercial and production wells, which includes seasonal variations in pumping.

We developed a set of future sea level and hydroclimate scenarios based on the latest climate change projections designed to predict worst-case saltwater intrusion in the Plymouth aquifers through 2100. Table 1 summarizes the predicted sea level rise under the highest scenario which includes major Antarctic ice sheet loss and about 180 cm of sea level rise. A monthly times series was developed by interpolating between decadal predictions through 2100 provided by Douglas and Kirshen (2022).

Table 1: Modeled sea level rise scenarios through 2100 showing the increase in sea level relative to the 2020 baseline.

Scenario	2040	2060	2080	2100
Sea Level Rise High-End (Major Antarctic ice sheet loss)	21.8 cm	57.9 cm	111.9 cm	180.5 cm

There is a substantial amount of uncertainty that remains in global climate projections regarding the predicted changes in precipitation patterns over the coming decades. Most of them predict this

region will become wetter overall, but the magnitude and seasonality of that change still has a large range of potential outcomes. These scenarios include the wettest overall outcome for the region and also the driest overall outcome. The changes in the drier scenario are primarily reflected in large decreases in Summer and Fall precipitation which can have major short-term impacts on the groundwater hydrology of the region.

We took a similar approach to sea level in identifying the driest hydroclimate projection (10th percentile probability) over the model domain through 2100 from Douglas and Kirshen (2022) (Table 2). We chose the driest projection because this allows us to predict worst-case saltwater intrusion from hydroclimate changes; with less terrestrial recharge, the freshwater-saltwater interface shifts landward. For terrestrial recharge, we did not use a specific scenario, but an overall 15% reduction in recharge from baseline values to reflect these projections. The four simulations presented in this document are in Table 3. Initial hydraulic head and TDS distributions for the simulations were identified by running a baseline simulation with constant model forcings until hydraulic head and TDS reached dynamic steady-state. We then ran each simulation with transient model forcings.

Table 2: Precipitation changes scenarios (reflected as recharge in the model) through 2100 showing the percentage change in precipitation relative to the 2020 baseline.

RCP 8.5 Emissions dry end-member	**2040**	**2060**	**2080**	**2100**
Winter (DJF)	+2.4 %	+4.5%	+5.5%	+6.4%
Spring (MAM)	+0%	+0.6%	+3.1%	+5.5%
Summer (JJA)	-3.3%	-7.5%	-14.5%	-21.6%
Fall (SON)	-3.8%	-7.4%	-10.7%	-14.0%

Table 3: Simulations and their respective flow model environmental and anthropogenic forcings.

Simulation	**Flow Model Forcings**
Simulation 1 (All Forcings)	Terrestrial recharge (baseline constant), well pumping (time-dependent), centralized wastewater re-infiltration (time-dependent), septic return flow (time-dependent), & high-end sea level rise (time-dependent)
Simulation 2 (No Septic Return Flow)	Terrestrial recharge (baseline constant), well pumping (time-dependent), centralized wastewater re-infiltration (time-dependent), & high-end sea level rise (time-dependent)
Simulation 3 (Only SLR & Recharge)	Terrestrial recharge (baseline constant) & high-end sea level rise (time-dependent)
Simulation 4 (All Forcings - 15% Recharge Reduction)	Terrestrial recharge - 15% reduction (constant), well pumping (time-dependent), centralized wastewater re-infiltration (time-dependent), septic return flow (time-dependent), & high-end sea level rise (time-dependent)

Forward-Looking Simulation Results

Changes in TDS concentrations from 2020 to 2100 in Simulation 1 range from 0 to 17,516 mg/L and are mainly driven by sea level rise (Figure 11). The zone representing TDS increases of 1,000-10,000 mg/L is generally 100 m wide at the water table but can extend to ~500 m wide in coastal marsh and estuary environments in the northern region of the model domain. Between Manomet Heights and Sagamore Beach, this zone increases in width to ~300 m below elevations of -28 m. This zone also increases in width to ~200 m between South Duxbury and Ocean Bluff between elevations of -16 and -32 m. The zone representing TDS increases of 100-10,000 mg/L is generally 200 to 300 m wide at the water table but can extend to 300 to 700 m near Center Hill Pond and in coastal marsh and estuaries in the north of the domain.

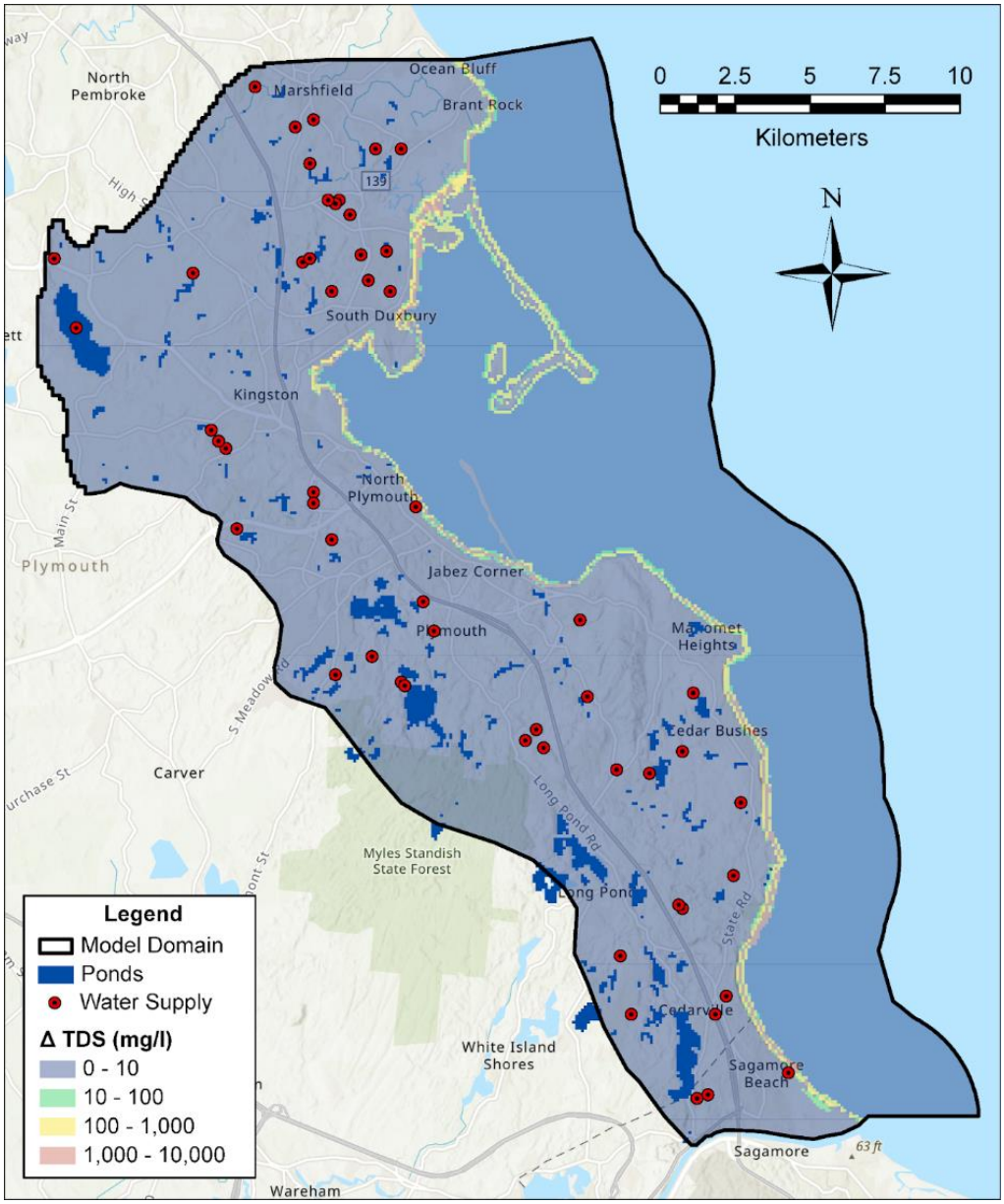

Figure 11: Concentration increase from 2020 to 2100 (Δ TDS) in Simulation 1 showing the landward migration of the interface mixing zone.

Coastal and stream discharge varies due to sea level rise throughout the model simulations. The total volume of water leaving the model through the RIV boundary increases by 6% between 2020 and 2100 (Figure 12a). Rising sea levels cause water table elevations to increase leading to an increase in groundwater discharge to surface water. Water leaving the model through the CHD boundary represents coastal groundwater discharge. Total coastal groundwater discharge decreases by 12% between 2020 and 2100 because as sea level rises and pumping increases, the hydraulic gradient between the ocean and the water table decreases (Figure 12b).

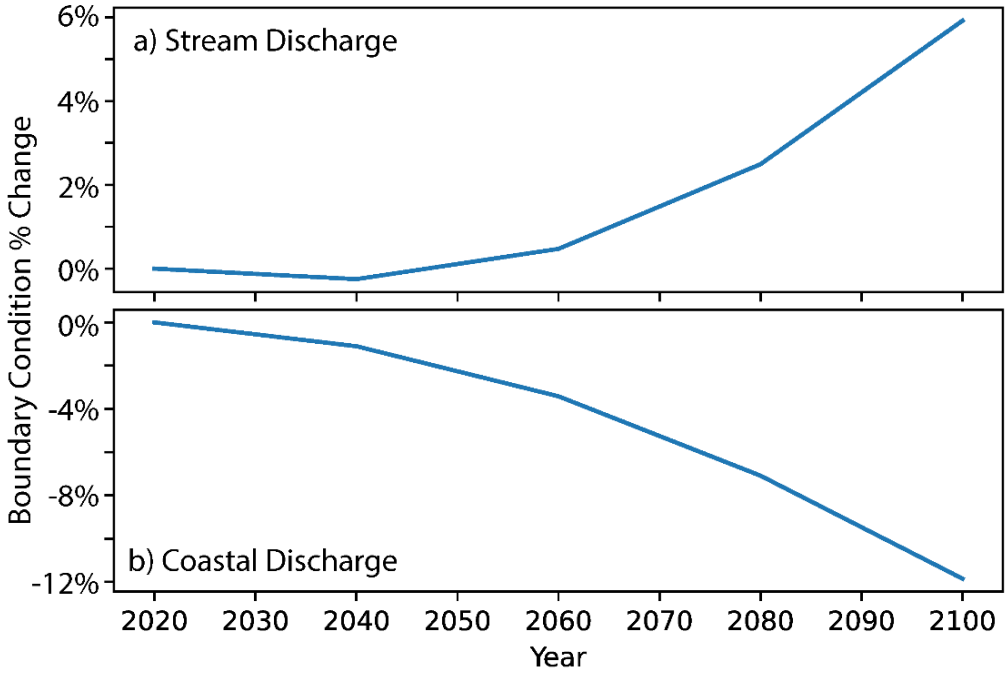

Figure 12: a) Percent change in total water volume leaving the model through the RIV boundary (a) and CHD boundary (b) in Simulation 1 from 2020 to 2100 at 20-year intervals.

We also evaluated the impacts of projected SLR, groundwater pumping, and terrestrial recharge on salinity in coastal ponds. For all simulations, the 2100 pond TDS values are less than 300 mg/L and within the EPA's safe limit for drinking (less than 500 mg/L). The locations of these ponds are shown in Figure 9. The model projects that salinity will increase in two ponds across all four simulations: Allens Pond and Scokes Pond (Figure 13). In general, both ponds are buffered by septic system re-infiltration when comparing Simulation 1 (all forcings) and Simulation 2 (no septic system re-infiltration). Both ponds increase in TDS by at least 6x more when reducing terrestrial recharge by 15% and keeping all other forcings the same (comparing Simulation 1 and Simulation 4), indicating that future terrestrial climate change could have a large impact on saltwater intrusion. The ponds show different sensitivities to pumping. Scokes Pond is more impacted by pumping; Simulation 2 has a larger TDS increase than Simulation 3 (no pumping or re-infiltration). Allens Pond is less sensitive to pumping as the TDS increase from Simulation 2 to Simulation 3 is only 2 mg/L. The likely explanation for this variability is the amount of pumping upgradient of these ponds; Scokes Pond has more upgradient pumping than Allens Pond.

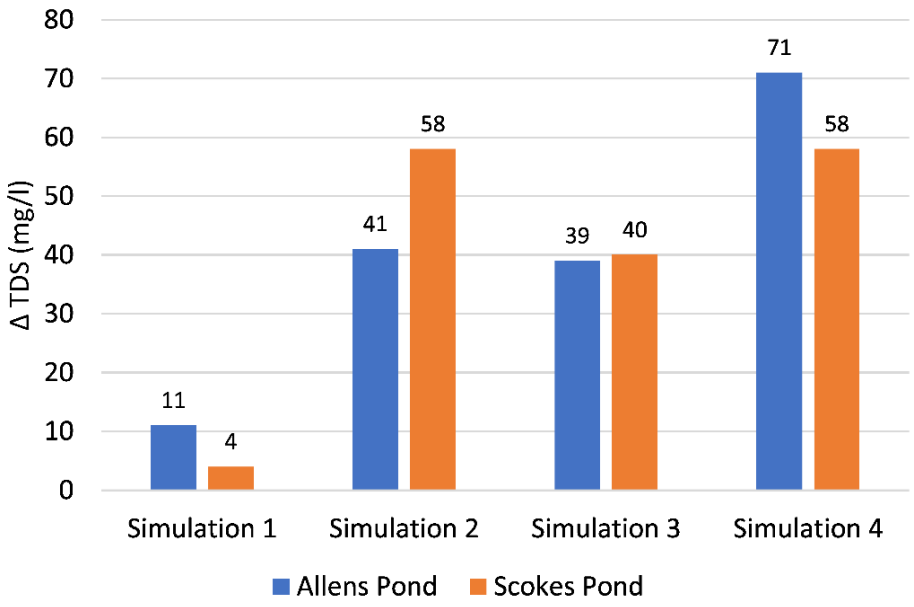

Figure 13: Concentration increase (Δ TDS) for Allens Pond and Scokes Pond from 2020 to 2100 for Simulation 1 (all forcings), Simulation 2 (no septic re-infiltration), Simulation 3 (no pumping or re-infiltration), and Simulation 4 (all forcings - 15% recharge reduction). See Figure 9 for the locations of these ponds.

Total dissolved solid concentrations in the year 2100 increase by 0 to 15,476 mg/L when reducing terrestrial recharge by 15% (2100 Simulation 4 TDS minus 2100 Simulation 1 TDS) (Figure 14). The 1,000-10,000 mg/L Δ TDS zone generally ranges from 100 to 200 m wide at the water table but can increase to ~700 m wide in coastal marsh and estuary environments in the northern region of the model. Salinity increases from reduced recharge occur because terrestrial hydraulic heads decrease with less recharge, so the hydraulic gradient between the saltwater and freshwater decreases allowing more saline water to flow landward.

Up-coning and lateral movement of the interface occurs at one well location within the model - DEP Well 4036002-02G. Figure 15 demonstrates how pumping causes increases in TDS in this well. Simulation 3 (green line) - no pumping or re-infiltration - has the lowest concentrations and smallest increase from 2020 to 2100 (77 mg/L), while Simulation 1 - all forcings - has larger concentrations and a larger increase from 2020 to 2100 (172 mg/L). The orange line - Simulation 2 with no septic system re-infiltration - has the largest concentrations and largest increase from 2020 to 2100 (430 mg/L), illustrating how septic system re-infiltration can buffer saltwater intrusion. The location and depth of this well in relation to mixing zone migration is shown in Figure 16. Well 4036002-02G (F-F') is 0 m from the freshwater-saltwater mixing zone, and model cells directly surrounding the well increased by 1 to 602 mg/L TDS from 2020 to 2100 in Simulation 1. The observed vs. simulated TDS for Well 4036002-02G were similar providing increased confidence that the elevated salinities in this well are from mixing zone saltwater intrusion; the average measured TDS value was 184 mg/L, and the simulated TDS value in 2020 was 229 mg/L (the average of the three cells within the screened interval). The Plymouth Water Supply Well (E-E') is 200 m from the freshwater-saltwater mixing zone, and model cells directly surrounding the well increased by ~0 mg/L TDS from 2020 to 2100.

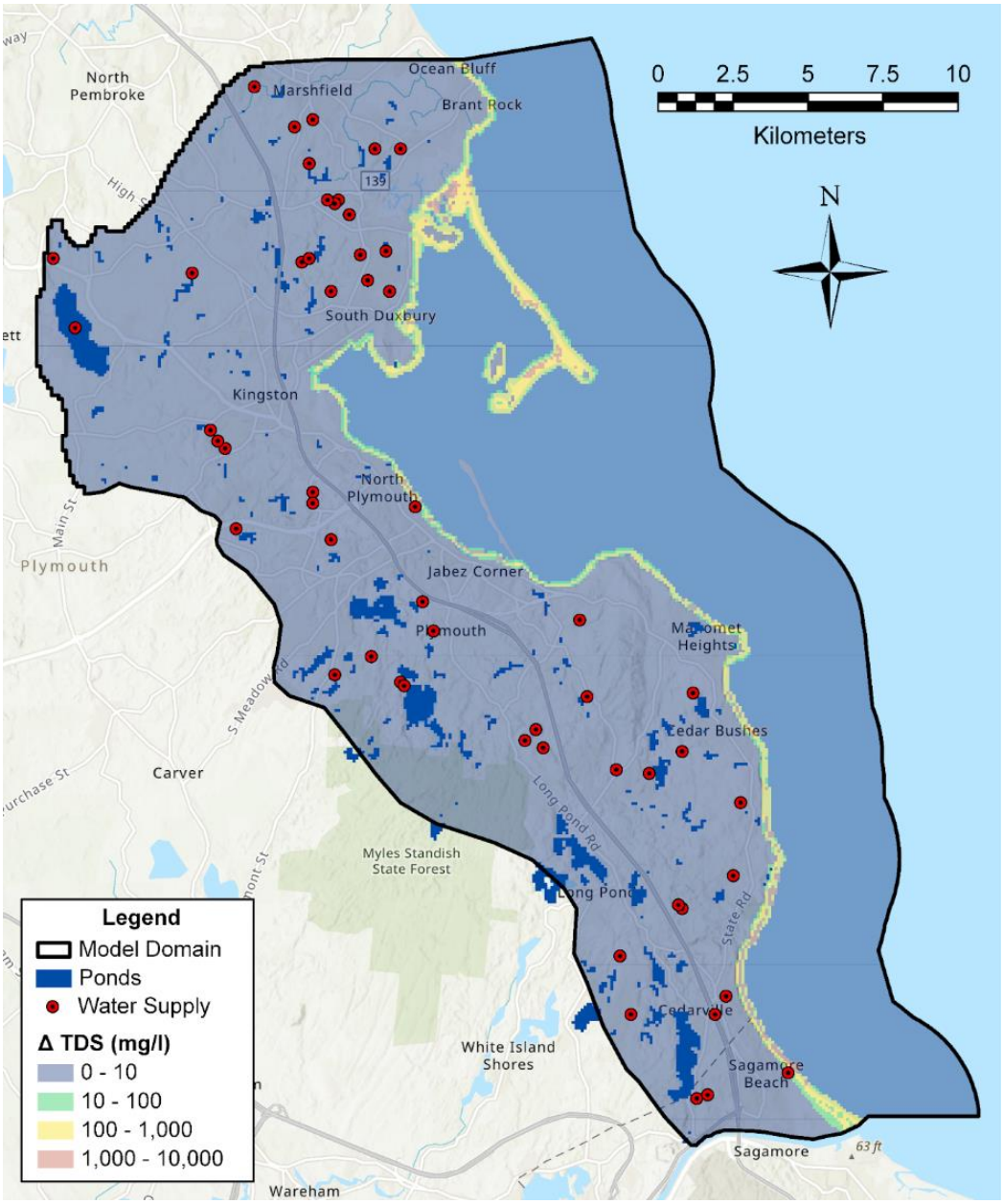

Figure 14: Concentration difference at year 2100 (Δ TDS) between Simulations 1 and 4 showing landward migration of the interface mixing zone from 15% reduction in terrestrial recharge.

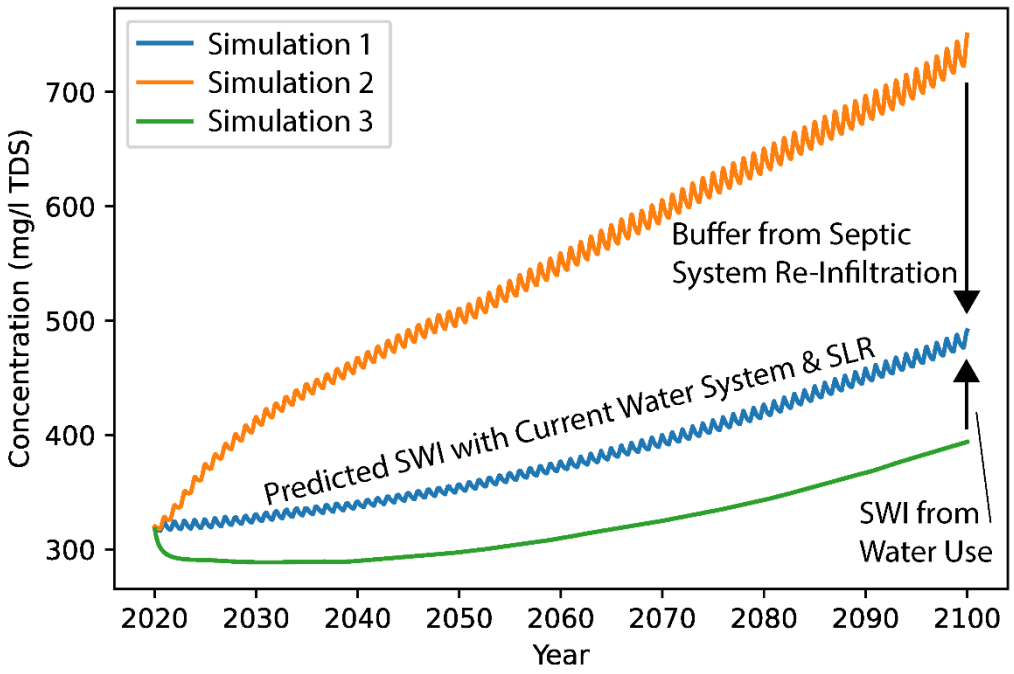

Figure 15: Simulated TDS concentrations from 2020 to 2100 being pumped from the bottom layer of the screened interval of DEP Well 4036002-02G, which extends through 3 model layers. Line color represents varying simulations: Simulation 1 (all forcings), Simulation 2 (no septic re-infiltration), and Simulation 3 (no pumping or re-infiltration).

The simulated hydraulic head was impacted by both sea level rise and pumping for Simulation 1 (Figure S3 and Figure S4). The head increase for the ocean was 1.8 m from 2020 to 2100 due to sea level rise in the CHD cells. This head increase propagates into the terrestrial aquifer system; the zone where terrestrial heads increased by at least 1 m ranges from ~400 m inland near Kingston and Duxbury to ~2 - 3 km inland near Manomet Heights and Brant Rock (Figure S3). This increase in hydraulic head is linked to the modern head gradient (Figure S2); where the head gradient was steepest, terrestrial head increases from sea level rise propagated less distance, and vice versa. Other locations where heads increased are centralized re-infiltration sites. Head decreases due to pumping are shown in Figure S4. The regions with the largest water table decrease from pumping are in the North Plymouth and Plymouth regions and at Silver Lake in the northwest of the model domain. The water pumped from Silver Lake is used by the City of Brockton public water supply. Although the impact of this drawdown is not directly quantified, these withdrawals do put the downgradient regions at greater risk of saltwater intrusion by reducing the flux of water to the coast.

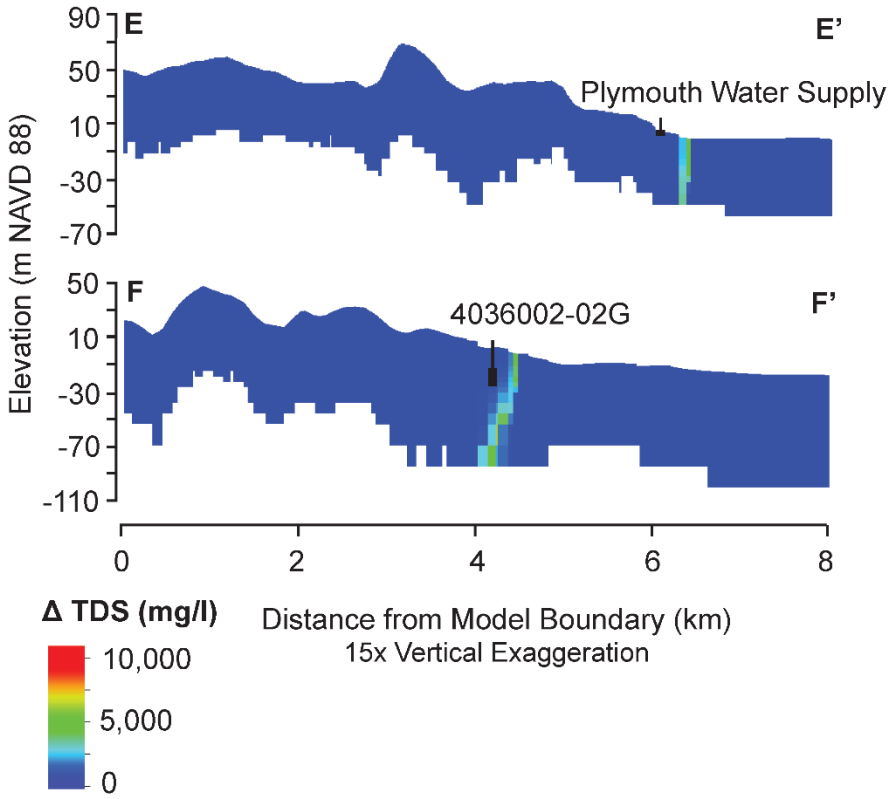

Figure 16: Cross-sections with the concentration increase from 2020 to 2100 (Δ TDS) in Simulation 1. Well screen intervals are shown as black rectangles. Locations of the cross-sections are shown in Figure 6.

Review of Hydrostratigraphy and Recommendations

Hydrostratigraphy and Geophysical Survey

Based on the groundwater flow and transport model some areas experience a higher probability of saltwater intrusion and are more likely to be impacted. Geophysical surveys are necessary to further quantify the risks coastal communities may be facing. Current knowledge of subsurface materials is limited. For this study, we analyzed well driller logs to identify if a coastal confining unit is present (Figure 17). Well logs are useful in characterizing grain size and soils. However, to create a more cohesive dataset that can be applied to climate resilience strategies, it would be beneficial to run an Airborne Electromagnetic Survey (AEM). This type of survey is performed by an instrument that is attached to a helicopter and flown across specific flight lines. The instrument transmits and receives electromagnetic waves. The response from the subsurface due to these waves is then measured to determine the electrical conductivity of the materials. Interpretation can be made to locate the freshwater-saltwater interface and coastal confining units that would affect saltwater intrusion and groundwater flow. In general, saltwater aquifers are highly conductive, freshwater aquifers are less conductive, bedrock has relatively low conductivity, and finer-grained units have higher conductivity.

The survey would run from about 1 km onshore to 2 km offshore. Initial subsurface investigations into the PCKD aquifer system showed some coastal silts and clays existed roughly seven meters onshore and into Plymouth Harbor (Hansen & Lapham, 1992). The location of where the Plymouth Carver sand and gravel aquifer extends offshore is not well characterized. Using AEM techniques, lithologies can be identified and the aquifer can be further mapped. In Monterey Bay, California, saltwater intrusion was mapped 3.5 km offshore with up to 18 m of depth resolution. The survey was able to penetrate through the conductive sea water and observe the underlying marine sediments. The saltwater-freshwater interface was identified because AEM data was able to show the water quality in offshore aquifers (Goebel et al., 2019).

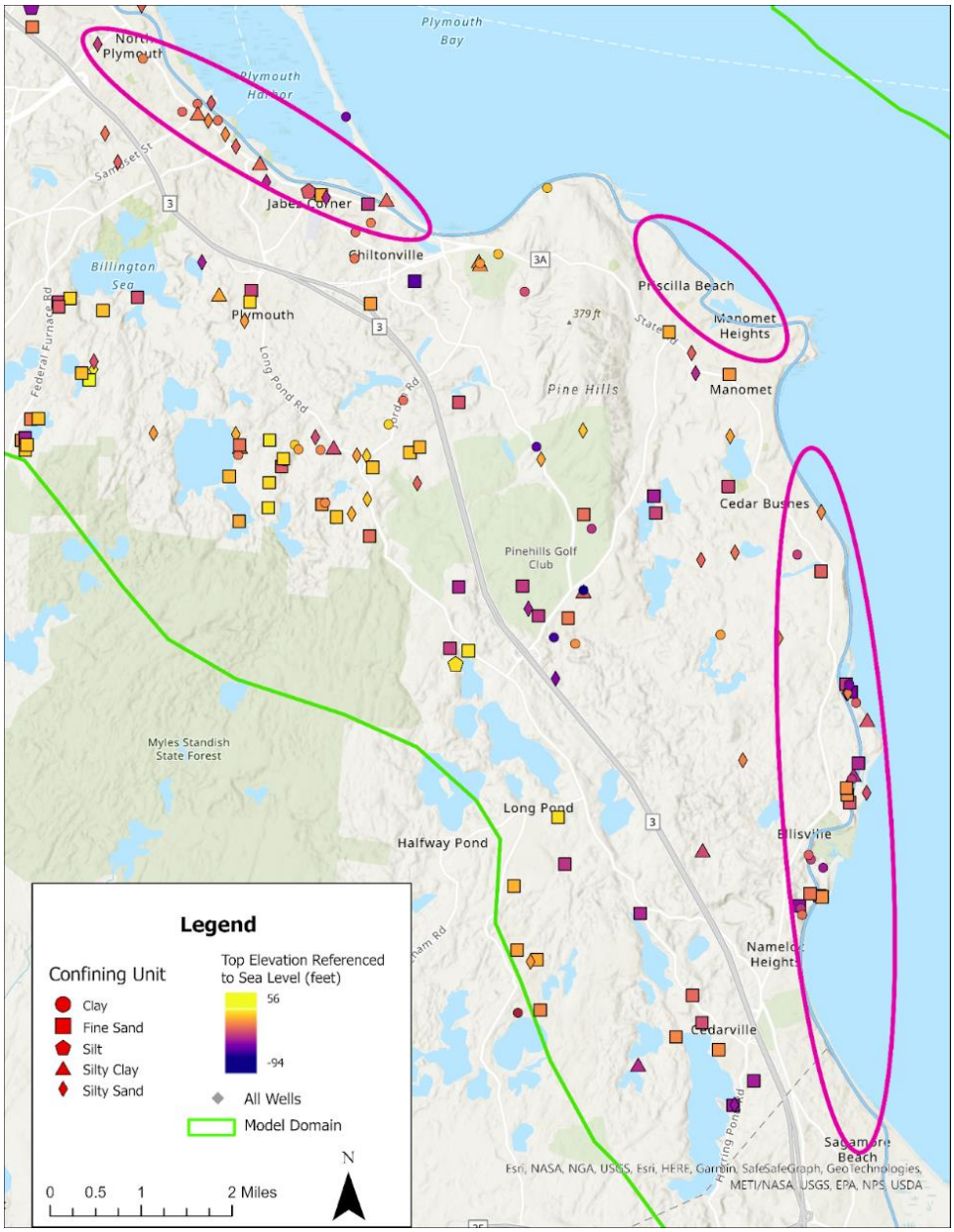

Figure 17: Map of wells that have a confining unit described in drillers logs (shape) and the associated top elevation of the unit (color). Key areas for geophysical investigation are shown as pink polygons.

Based on our existing findings, an AEM survey is a logical next step. Interpretation of AEM data requires ground truthing from well logs, surficial geology, and known water salinity. As part of the current project, there is a comprehensive salinity database that shows areas of confirmed high conductivity conditions. Flight lines can be designed to investigate wells with elevated salinities and target areas that are most susceptible to saltwater intrusion (noted in pink in Figure 17).

Early Warning System and Optimal Well Placement

The suggested locations for an early warning system for salinity monitoring due to sea level rise are shown in Figure 18. The wells should be nested piezometers (3 in total) screened at different depths

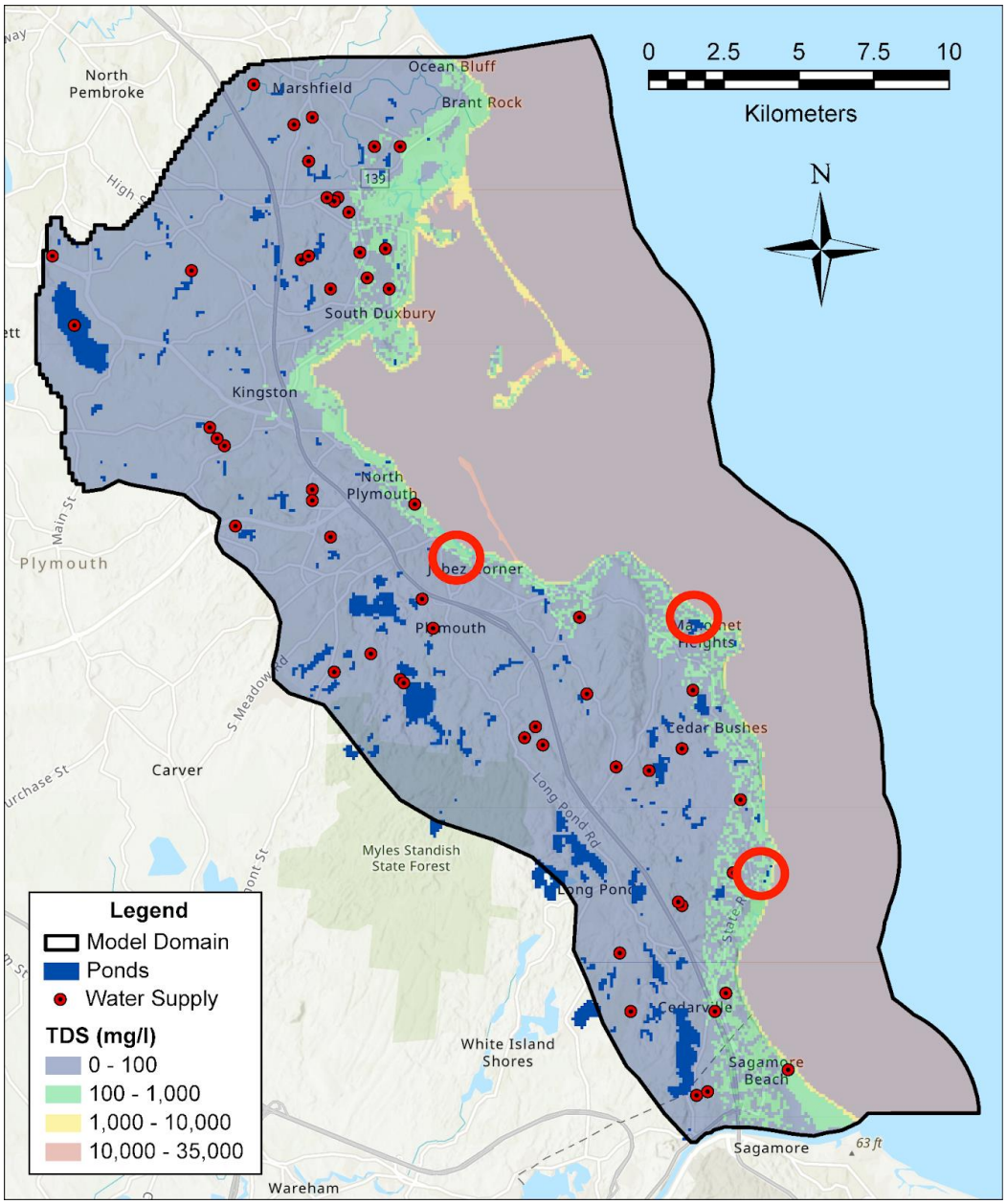

Figure 18: Map showing pond locations, water supply wells, and simulated total dissolved solids in relation to suggested locations (red circles) for salinity monitoring wells.

throughout the aquifer. Wells should be geophysically logged and completed using a professional hydrogeologist consultancy. Real-time pressure and salinity monitoring should be installed in the wells and maintained quarterly. These are also areas that could be subject to overwash events and would be helpful for monitoring the impacts of storms on near-surface aquifer salinity.

Figure 19 shows the current production well sites and capture zones for the region. We also show the simulated salinity zones of the aquifer. While the siting of wells is a complex process that involves land use, aquifer considerations, and logistical details - we suggest moving new public water supplies in the region outside of the green contours associated with TDS between 100-1,000 mg/L.

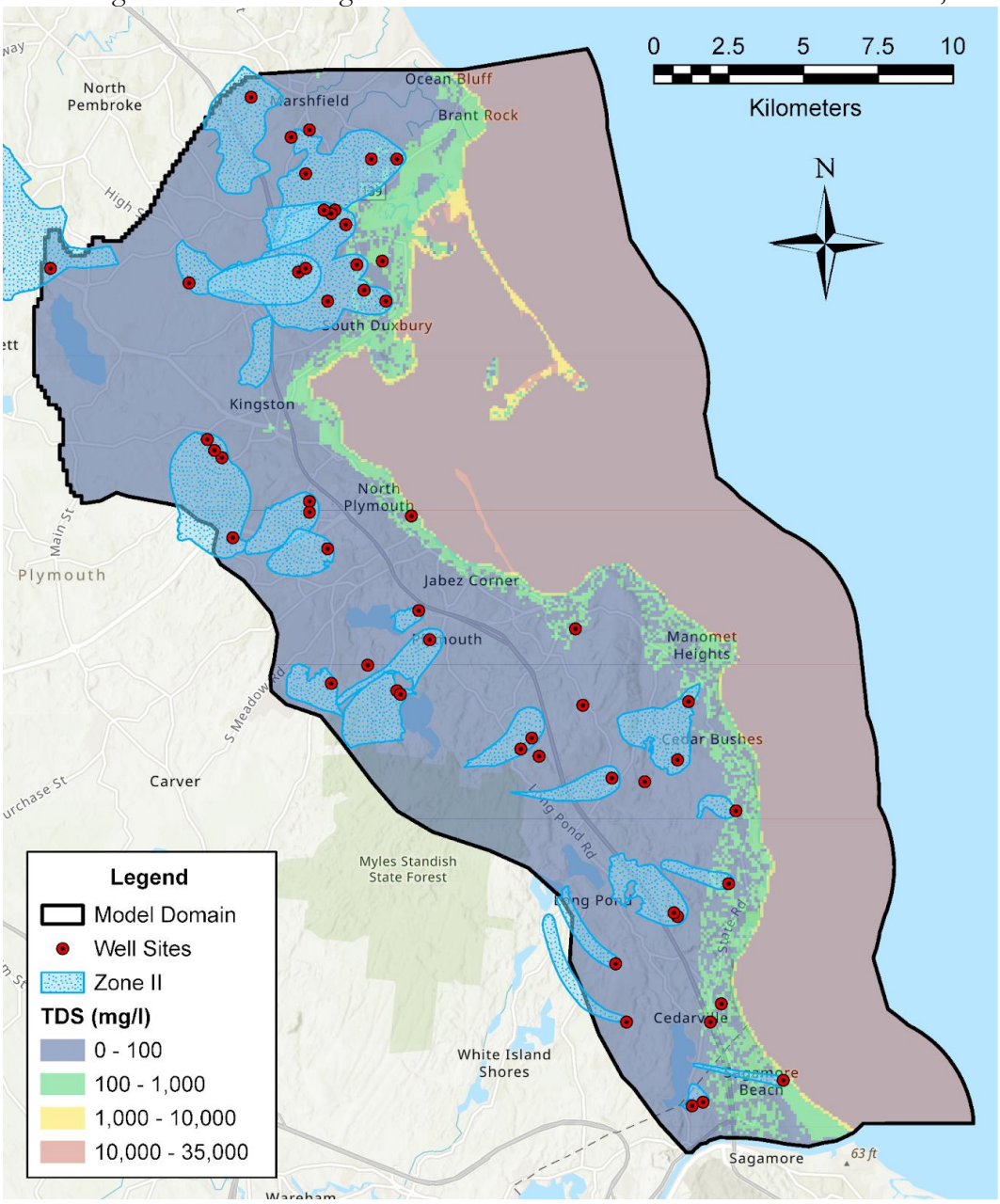

Figure 19: Map showing pond locations, water supply wells, and simulated total dissolved solids in relation to suggested criteria for locating new water supply development wells.

The forward-looking modeling presented above shows limited onshore migration (~200 meters) of the freshwater-saltwater interface. These scenarios looked at the migration due to subsurface migration of saltwater alone. These simulations do not account for storm surge, tidal processes, and other surface water inundation processes. The movement of coastal surface waters into freshwater ponds and streams is an additional important process to introduce saltwater into the shallow near-surface aquifer. Future studies should investigate surface water inundation into sensitive surface water features. There are existing efforts regionally to model impacts such as these including grounds at the Woodwell Climate Research Center and the University of Massachusetts Lowell. Therefore, monitoring of surface water salinity in key locations throughout the town is critical. Additionally, we are proposing several locations for subsurface salinity measurements to take place throughout the model domain and the town of Plymouth.

Based on the modeling results presented we have the following recommendations and suggestions:

- Develop and maintain a salinity database for surface and groundwaters across the town and create a public dashboard for open access to salinity observations in town water supply wells.
- Raise funds to perform an airborne electromagnetic geophysical survey of coastal areas to image the extent of saltwater intrusion (to test modeling) and document the hydrostratigraphic architecture of key coastal areas.
- Develop an early warning system for subsurface salinity changes in key coastal areas (see Figure 18).
- Consider the suggested recommendations in Figure 19 for the optimal placement of freshwater production wells.

Actions to continue to control salinity intrusion into the aquifer:

- Continue to re-infiltrate wastewater into the onshore aquifer system.
- Reduce overall freshwater pumping and encourage water-use reductions.
- Limit the extent of saltwater intrusion into surface water bodies - as this represents quick pathways for subsurface infiltration of saltwater into the aquifer

Conclusion

We developed a salinity database to define current (1980 - 2023) salinity distributions in groundwater and surface water. All average TDS concentrations for public water supply wells were within the EPA's safe drinking water recommendation (less than 500 mg/L). Two non-PWS wells (630 and 640 mg/L) and four surface water locations (636 to 1688 mg/L) had concentrations above the safe drinking water recommendation. The sources of elevated TDS were likely road salt and human development as these locations are relatively far from the freshwater-saltwater mixing zone, although further studies are required to improve our understanding of salinity sources.

The groundwater flow and transport model provided insights on both modern salinity distributions and predicted saltwater intrusion through 2100 in the Plymouth aquifer. The modern mixing zone (1,000 to 10,000 mg/L TDS) was 100 to 200 meters wide at the water table. The model simulations predicted the mixing zone would migrate 100 to 500 meters inland and aquifer salinities would increase by 0 to 17,000 mg/L by 2100 due to sea level rise and pumping. Based on modern (2023) and simulated pond concentrations, Allens Pond, Scokes Pond, and Center Hill Pond are most at risk of TDS increases due to saltwater intrusion; these ponds are at low elevations (1 to 3 m) and

close to the coast (less than 150 m). Model simulations identified one pumping well to be at risk of future elevated TDS concentrations: DEP Well 4036002-02G. This well is ~300 m from the coast with a modeled screen elevation of -12 to -24 m. Variations in pond and well concentrations from the four simulations show that septic system re-infiltration (assuming a TDS concentration the same as recharge) buffers saltwater intrusion. We also find that terrestrial recharge plays an important role in limiting saltwater intrusion; compared to simulations with modern recharge rates, the mixing zone was predicted to migrate 100 to 700 meters further inland by 2100 with a 15% reduction in recharge. To best control saltwater intrusion, we suggest that Plymouth maintain a salinity database for surface water and groundwater, continue to re-infiltrate wastewater into the onshore aquifer system, encourage water-use reductions, and limit the extent of saltwater intrusion into surface water bodies.

References

Andrews, B.D., Baldwin, W.E., Sampson, D.W., and Schwab, W.C., 2018, Continuous bathymetry and elevation models of the Massachusetts coastal zone and continental shelf (ver. 3.0, December 2019): U.S. Geological Survey data release, https://doi.org/10.5066/F72806T7.

Bosserelle, A. L., Morgan, L. K., & Hughes, M. W. (2022). Groundwater rise and associated flooding in coastal settlements due to sea-level rise: a review of processes and methods. *Earth's Future*, *10*(7), e2021EF002580.

Douglas, E. and Kirshen, P., 2022, Climate Change Impacts and Projections for the Greater Boston Area.

Goebel, M., Knight, R., & Halkjær, M., 2019, Mapping saltwater intrusion with an airborne electromagnetic method in the offshore coastal environment, Monterey Bay, California. Journal of Hydrology: Regional Studies, 23, 100602.

Hansen, B.P. and Lapham, W.W., 1992, Geohydrology and simulated ground water flow, Plymouth-Carver aquifer, southeastern Massachusetts: Water-resources investigations report 90-4204.

Hem, J. D. (1985). *Study and interpretation of the chemical characteristics of natural water* (Vol. 2254). Department of the Interior, US Geological Survey.

Kaushal, S. S., Likens, G. E., Pace, M. L., Reimer, J. E., Maas, C. M., Galella, J. G., ... & Woglo, S. A. (2021). Freshwater salinization syndrome: From emerging global problem to managing risks. *Biogeochemistry*, *154*, 255-292.

Langevin, C.D., Hughes, J.D., Provost, A.M., Russcher, M.J., Niswonger, R.G., Panday, Sorab, Merrick, Damian, Morway, E.D., Reno, M.J., Bonelli, W.P., and Banta, E.R., 2023, MODFLOW 6 Modular Hydrologic Model version 6.4.2: U.S. Geological Survey Software Release, 28 June 2023, https://doi.org/10.5066/P9FL1JCC.

Mabee, S.B., W.P. Clement, C. Duncan, M. Pope, K. Moynahan, R. Miller, H. Davis and A. Low, 2022, A data set of depth to bedrock described in drill holes and geophysical surveys for Massachusetts - Release 1. Massachusetts Geological Survey Data Release DR22-01. Spreadsheet, metadata and 15-page report.

Masterson, J.P., Carlson, C.S., and Walter, D.A., 2009, Hydrogeology and simulation of groundwater flow in the Plymouth-Carver-Kingston-Duxbury aquifer system, southeastern Massachusetts: U.S. Geological Survey Scientific Investigations Report 2009–5063, 110 p.

Rusydi, A. F. (2018, February). Correlation between conductivity and total dissolved solid in various type of water: A review. In *IOP conference series: earth and environmental science* (Vol. 118, p. 012019). IOP Publishing.

Stone, B.D., and Stone, J.R., 2019, Geologic Origins of Cape Cod, Massachusetts; Guidebook for the Northeast Friends of the Pleistocene, 82nd Annual Fieldtrip, May 31-June 2, 2019: Massachusetts Geological Survey Open-file Report 19-01, 63 p.

Supplemental Information

Table S1: Hydrogeologic units defined in Masterson et al. (2009) with calibrated horizontal hydraulic conductivity (K) from this study.

Hydrogeologic Unit	K (m/day)
Medium to coarse sand & fine to coarse gravel	9.1 - 76.2
Stratified Drift	1.5 - 76.2
Coastal Unit (sand)	30.5
Upper unit of well-sorted fine gravel and medium to coarse sand 15 to 20 ft thick, middle unit of fine to coarse sand and some pebble gravel, and lower unit of fine sand and silt and clay of variable thickness. Mantles sand and gravel beneath parts of Plymouth kamefield.	45.7
Fine sand, overlying silt and clay generally 10 to about 50 ft thick. In Plymouth, kamefield deposits may lie above stratified sand and gravel; at southern border of Carver outwash, plain deposits lie on compact till or on coarse, bouldery ablation deposits.	12.2
Loose, unsorted, unstratified, bouldery silty sandy gravel (sandy till) less than 30 ft thick that mantles fine to coarse sand containing some beds of sandy gravel. North of Ellisville Moraine in Manomet, underlying sand contains a relatively thin zone of compact till and rests on basal compact till.	20.5 - 36.2
Loose, unstratified, unsorted sandy silty gravel (sandy till); poorly stratified and poorly sorted coarse sandy boulder gravel containing some well stratified, well sorted sandy gravel.	15.9 - 64.5
Bedrock	4.9

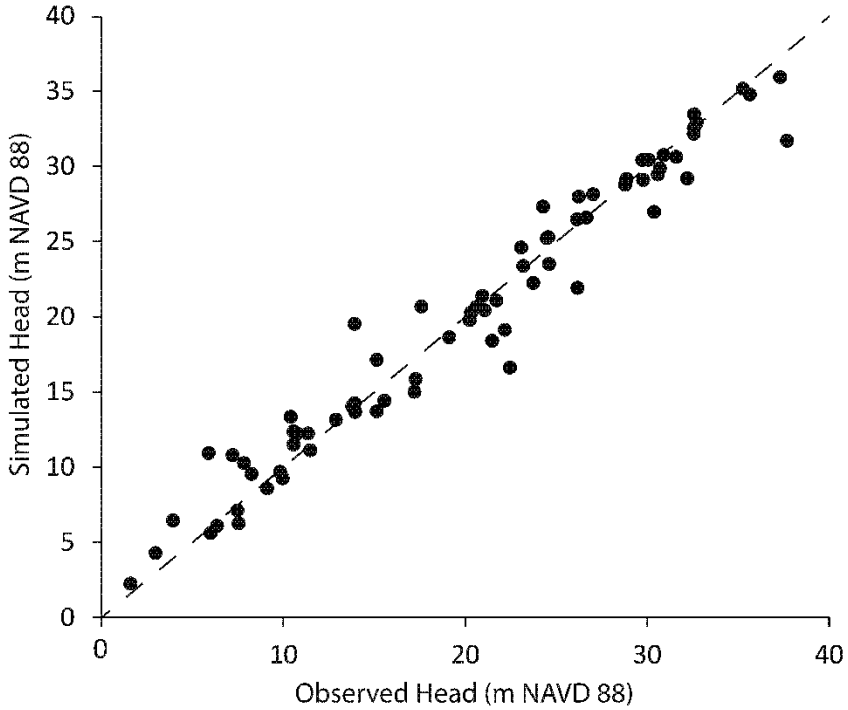

Figure S1: Observed vs. simulated heads for the baseline simulation.

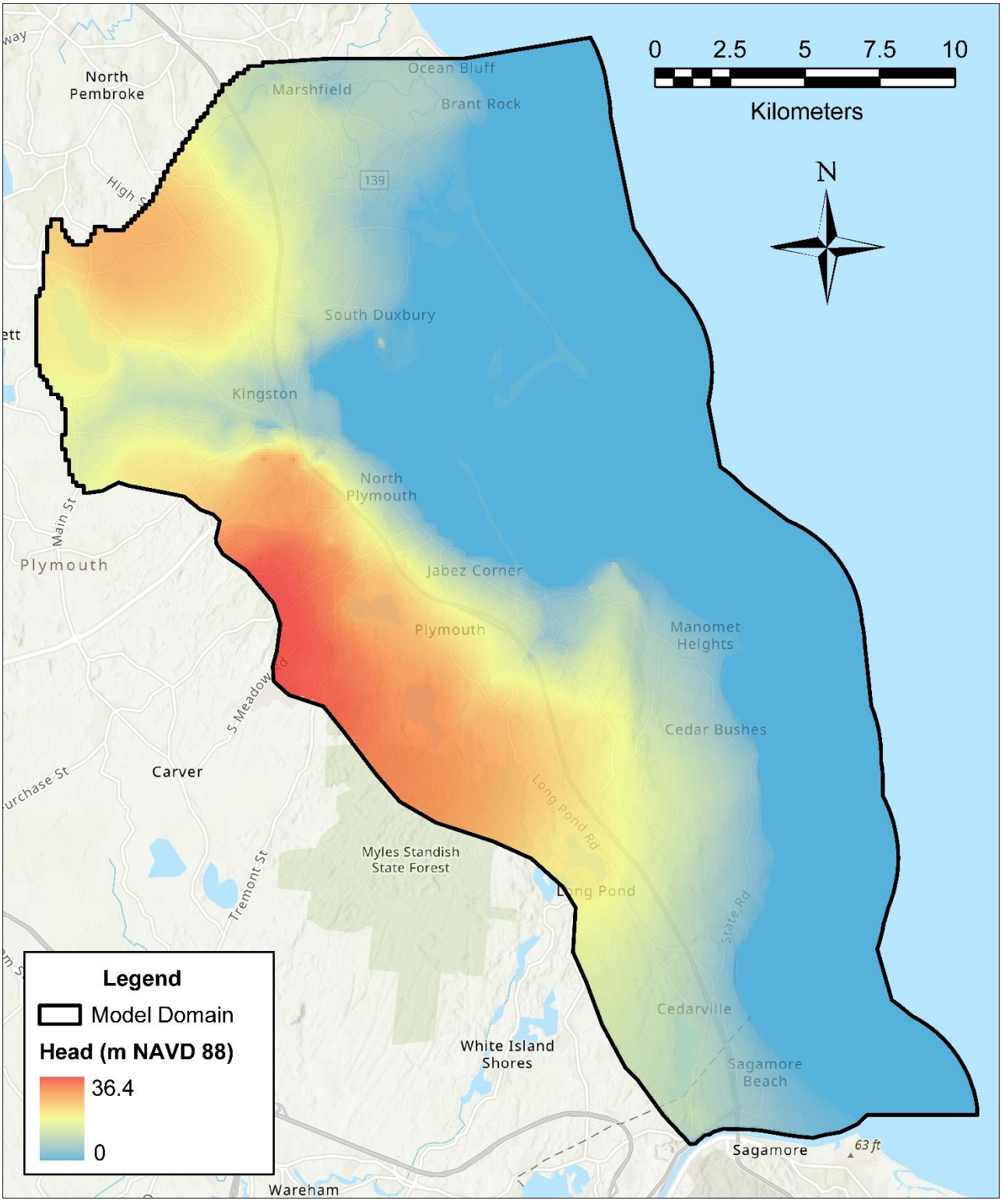

Figure S2: Modern (2023) simulated hydraulic heads at the water table for Simulation 1 in meters NAVD 88.

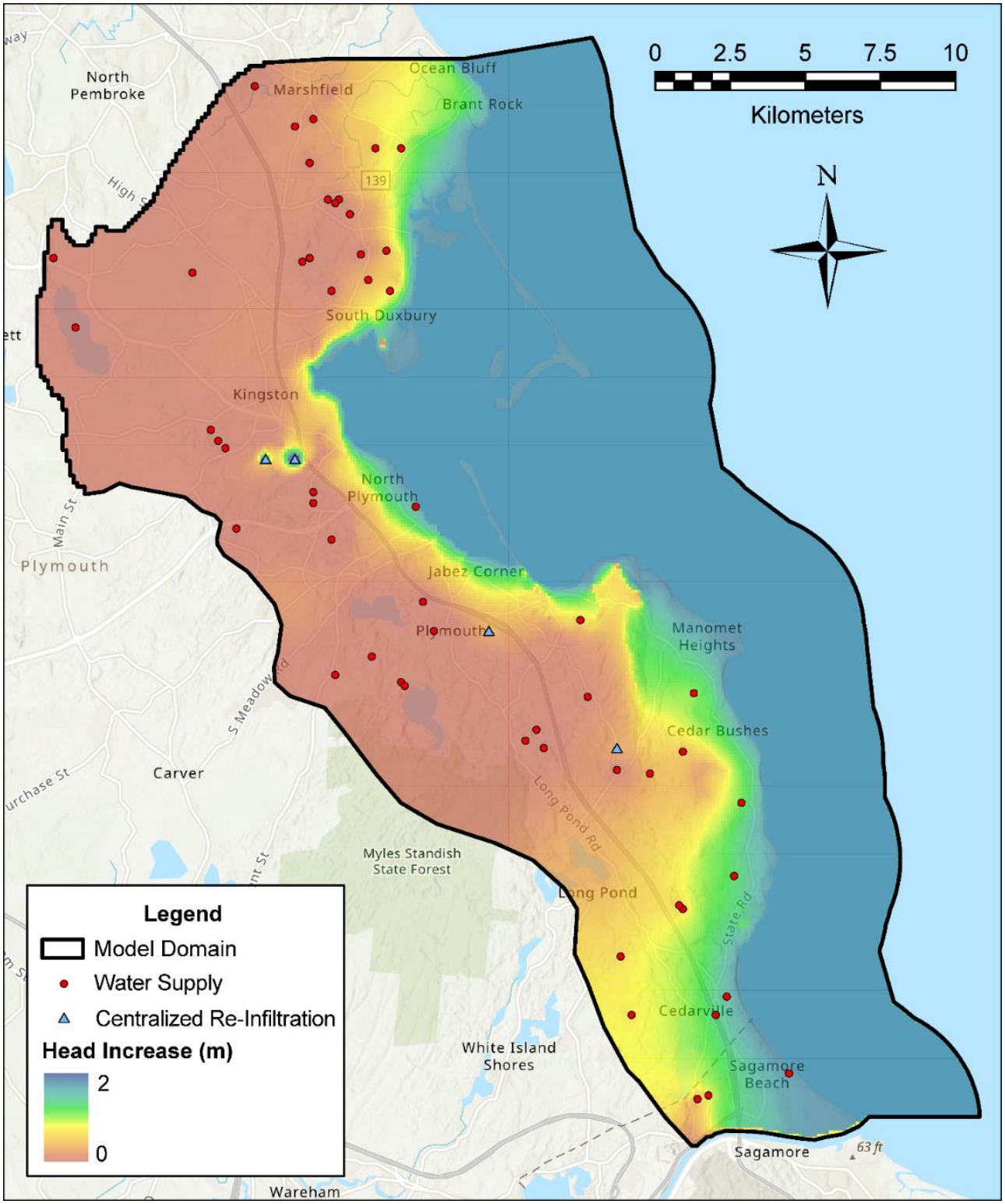

Figure S3: Increase in head (meters) from 2020 to 2100 for Simulation 1.

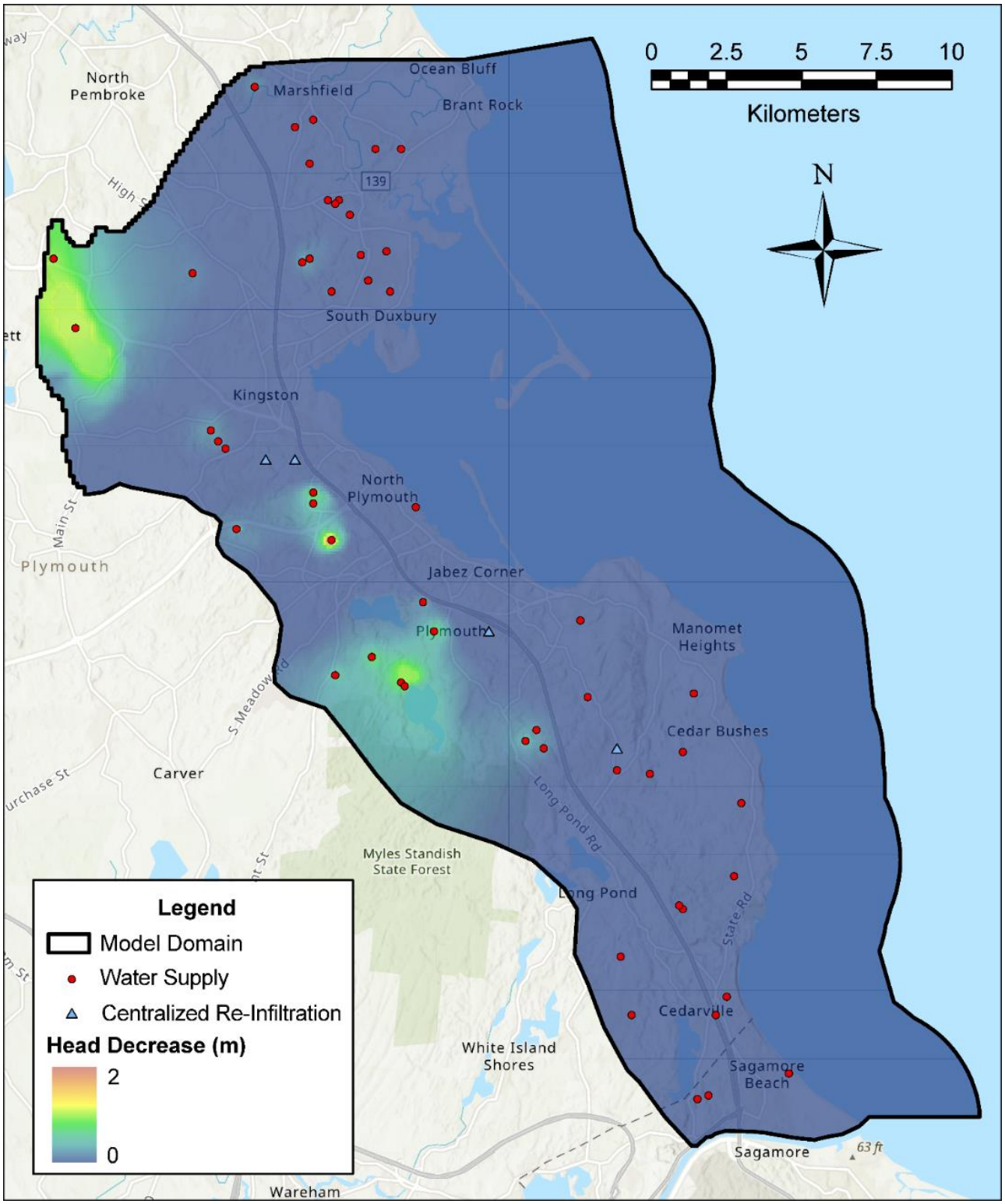

Figure S4: Decrease in head (meters) from 2020 to 2100 for Simulation 1.

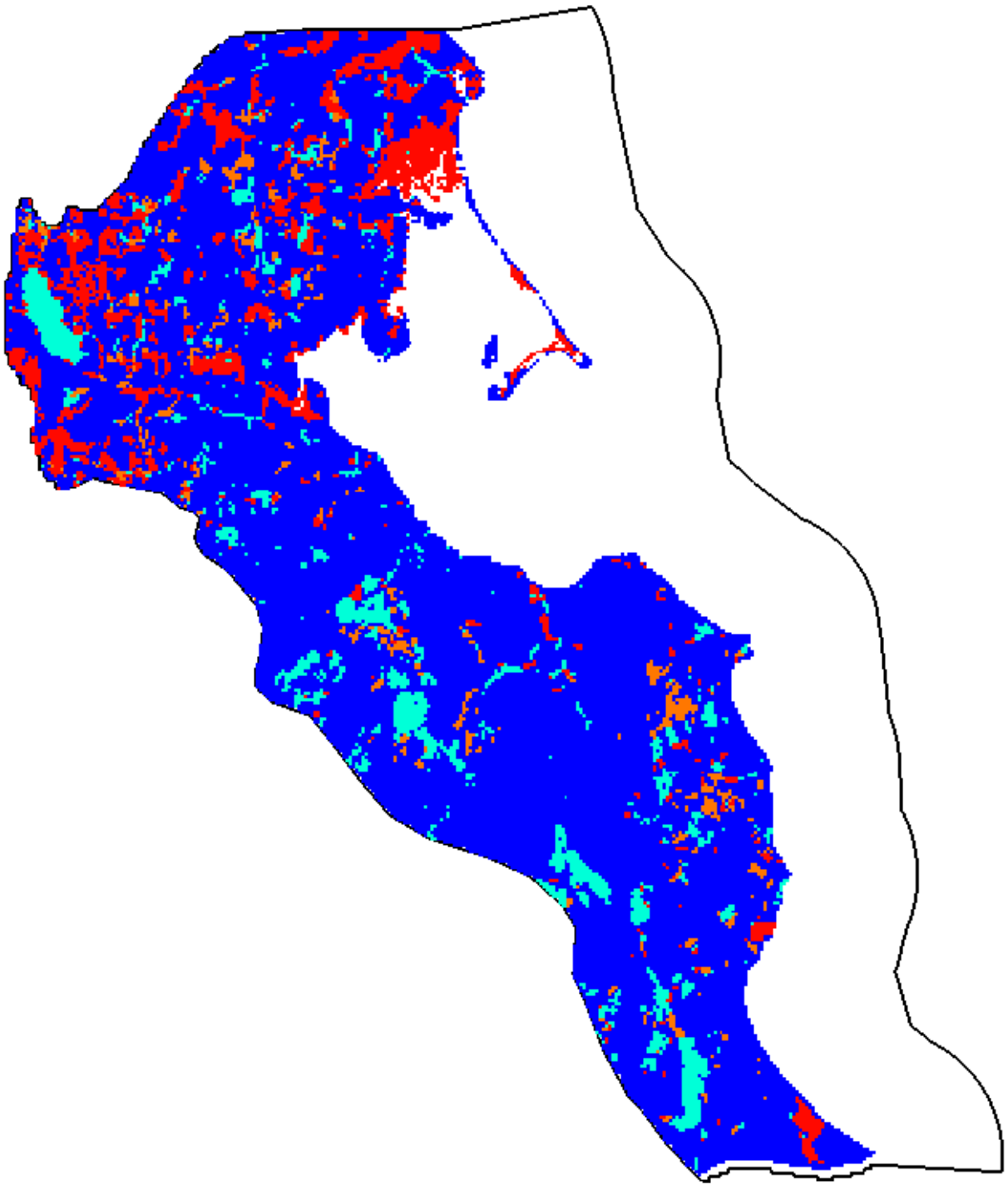

Figure S5: Location of model cells with RCH boundary condition for terrestrial recharge. Colors represent variations in recharge rate.

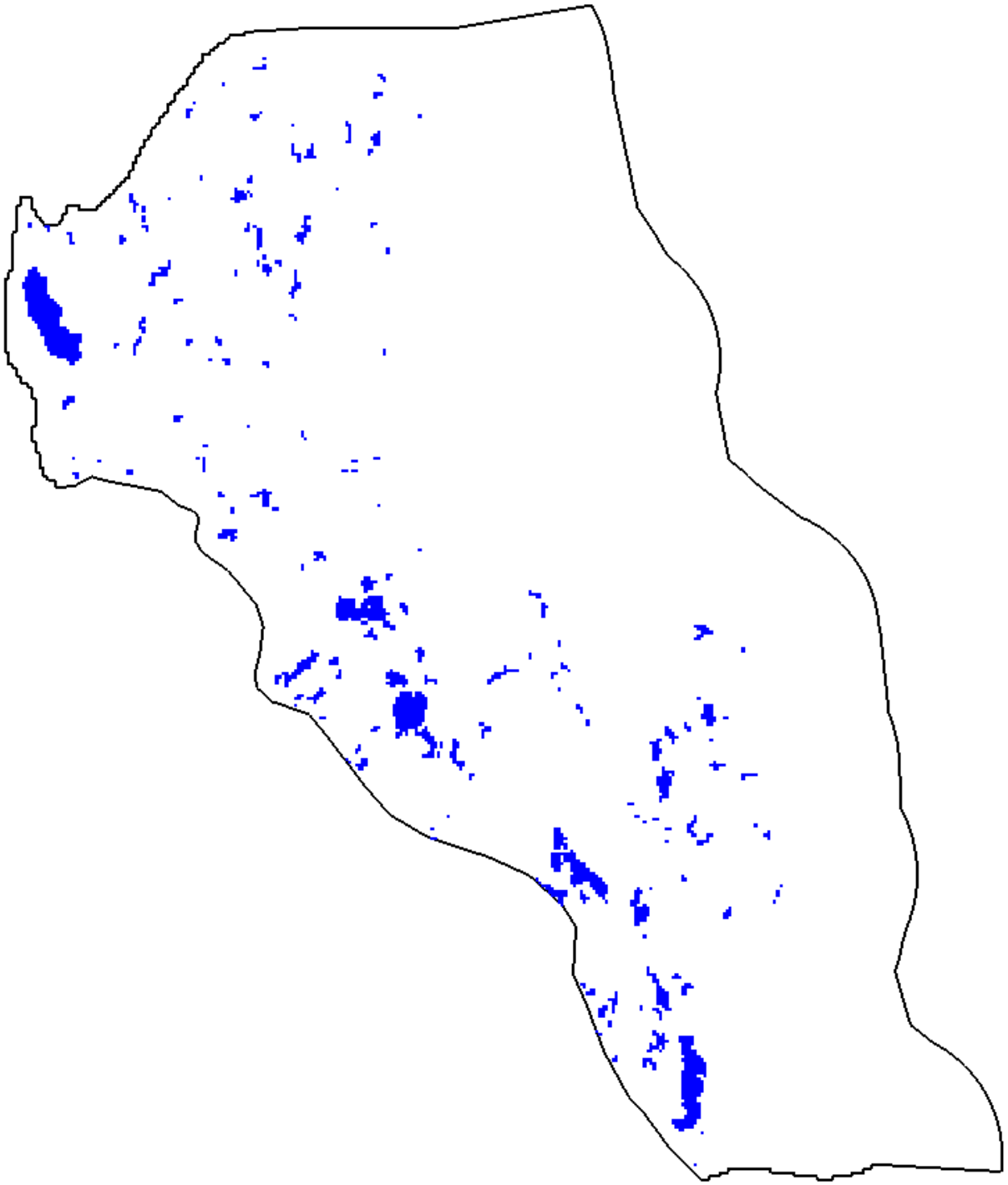

Figure S6: Location of model cells with ponds (high hydraulic conductivity).

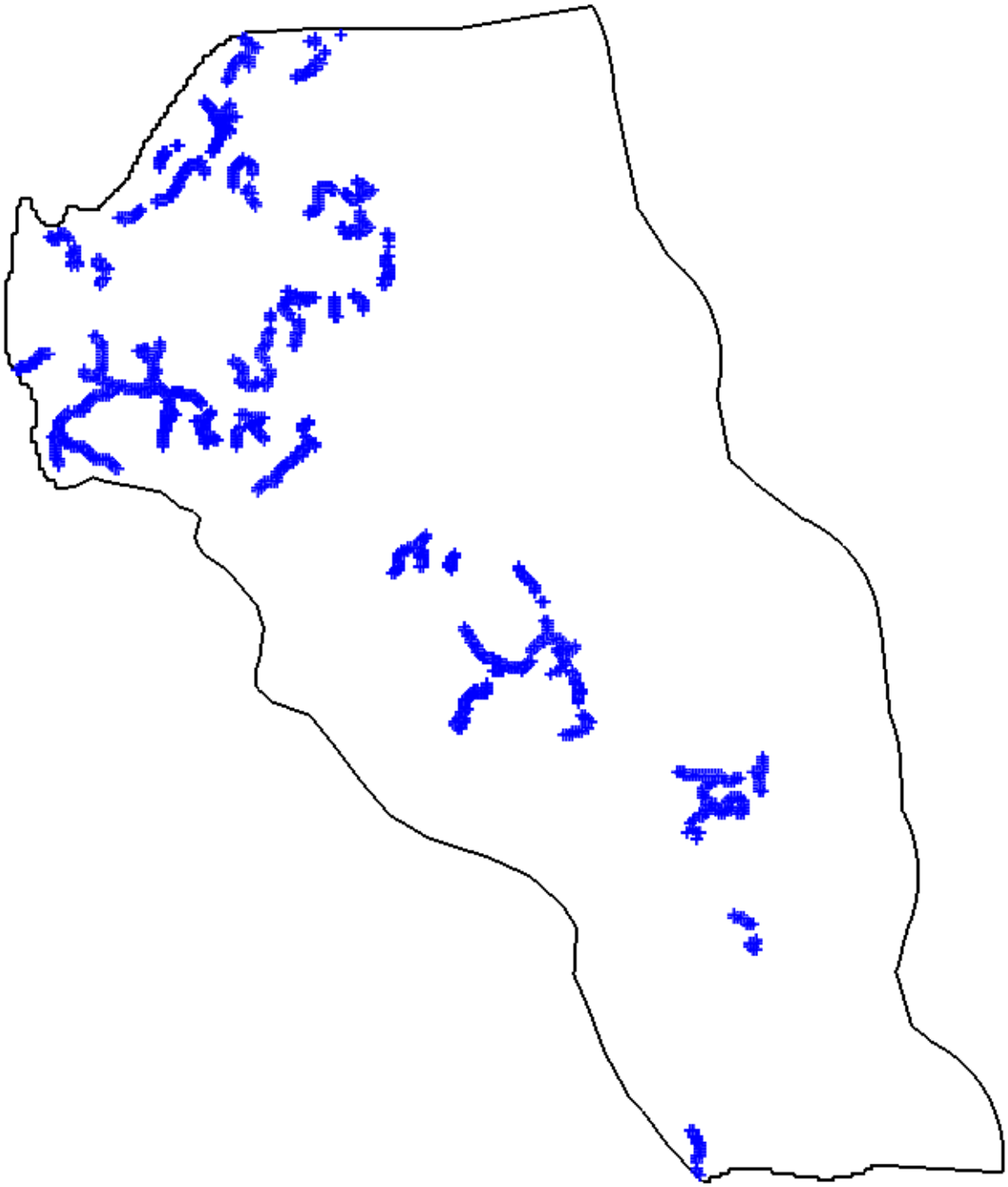

Figure S7: Location of model cells with RIV boundary condition.

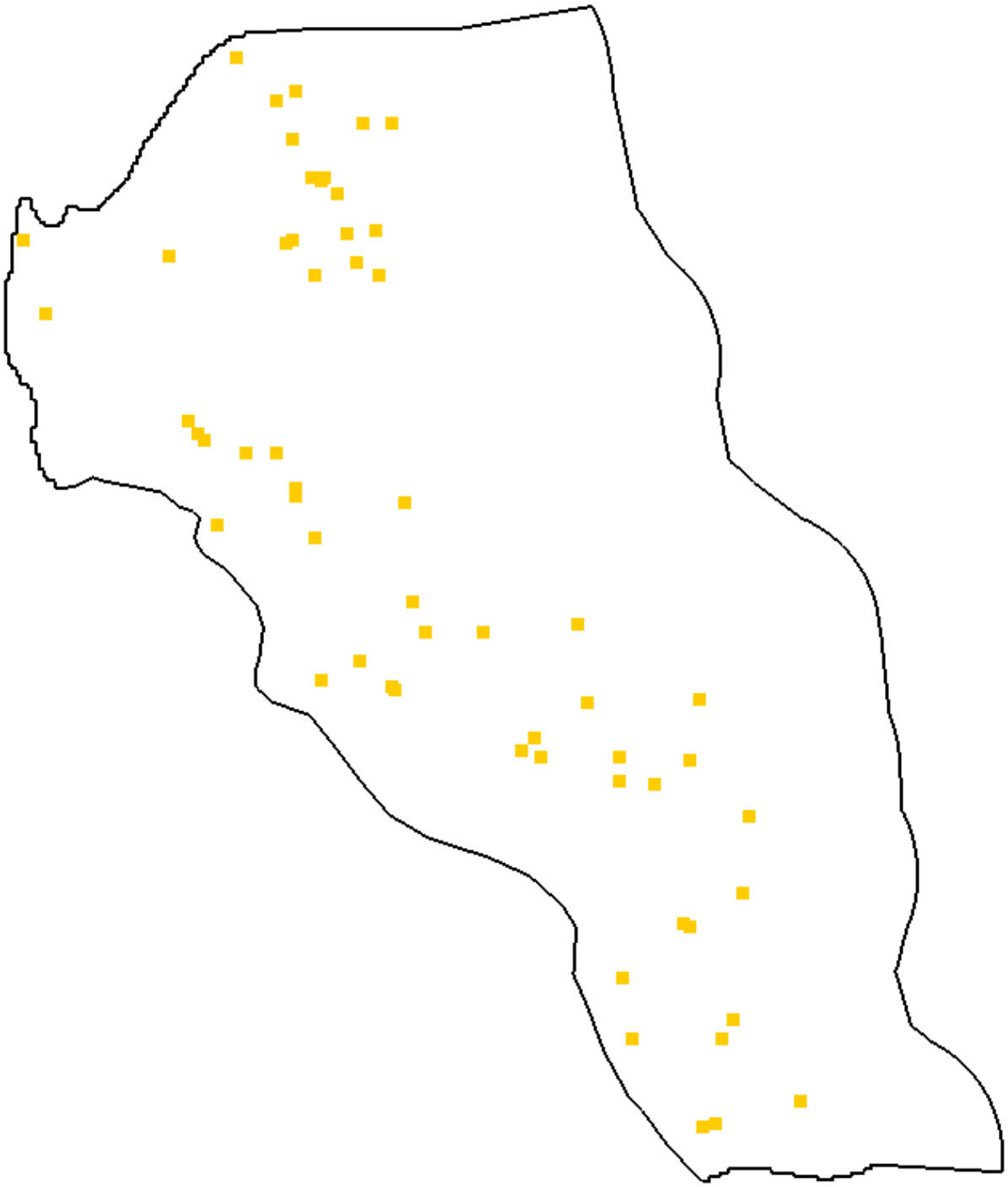

Figure S8: Location of model cells with WEL boundary condition.

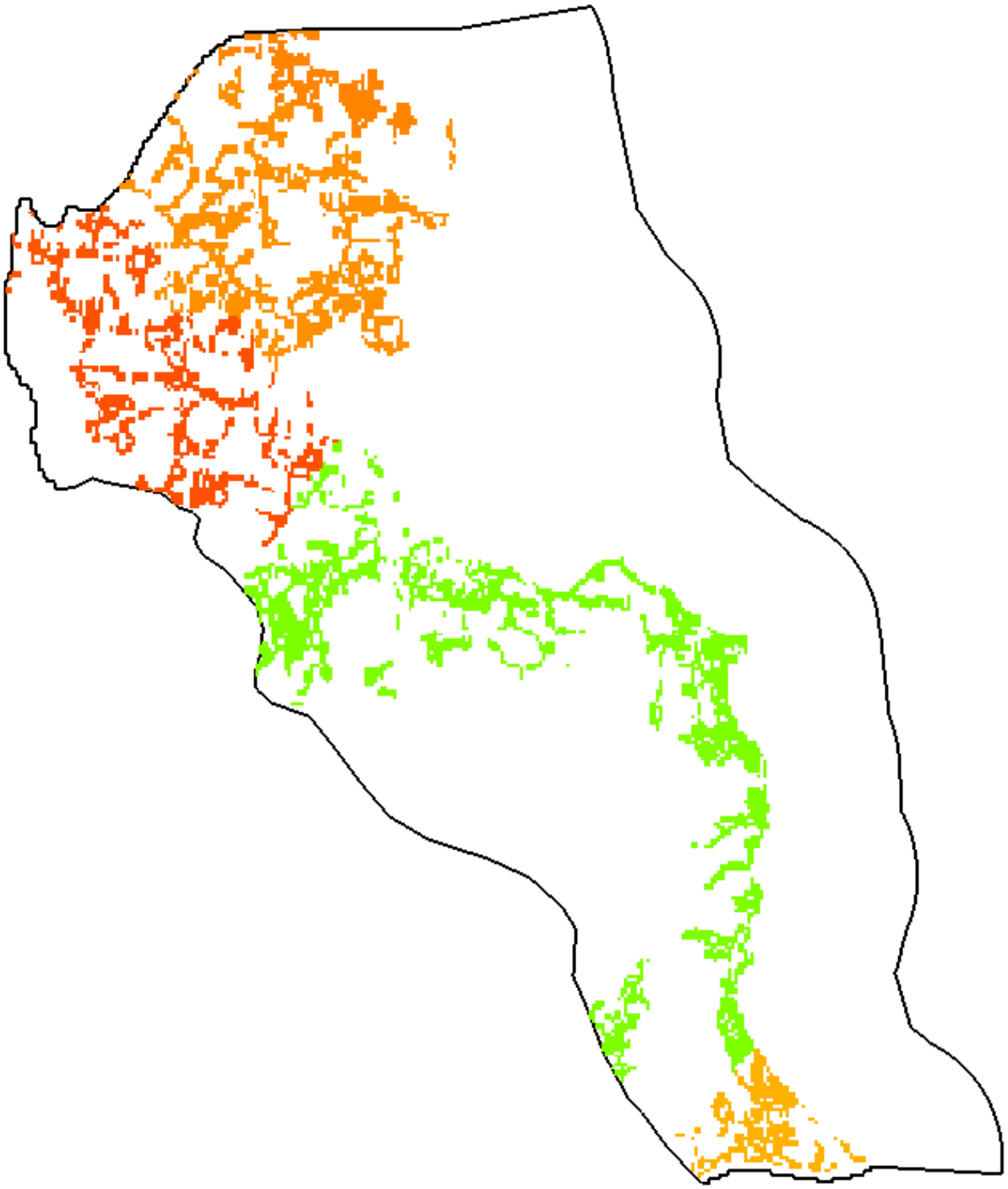

Figure S9: Location of model cells with RCH boundary condition for septic system return flow. The colors represent the 6 zones of septic system re-infiltration.

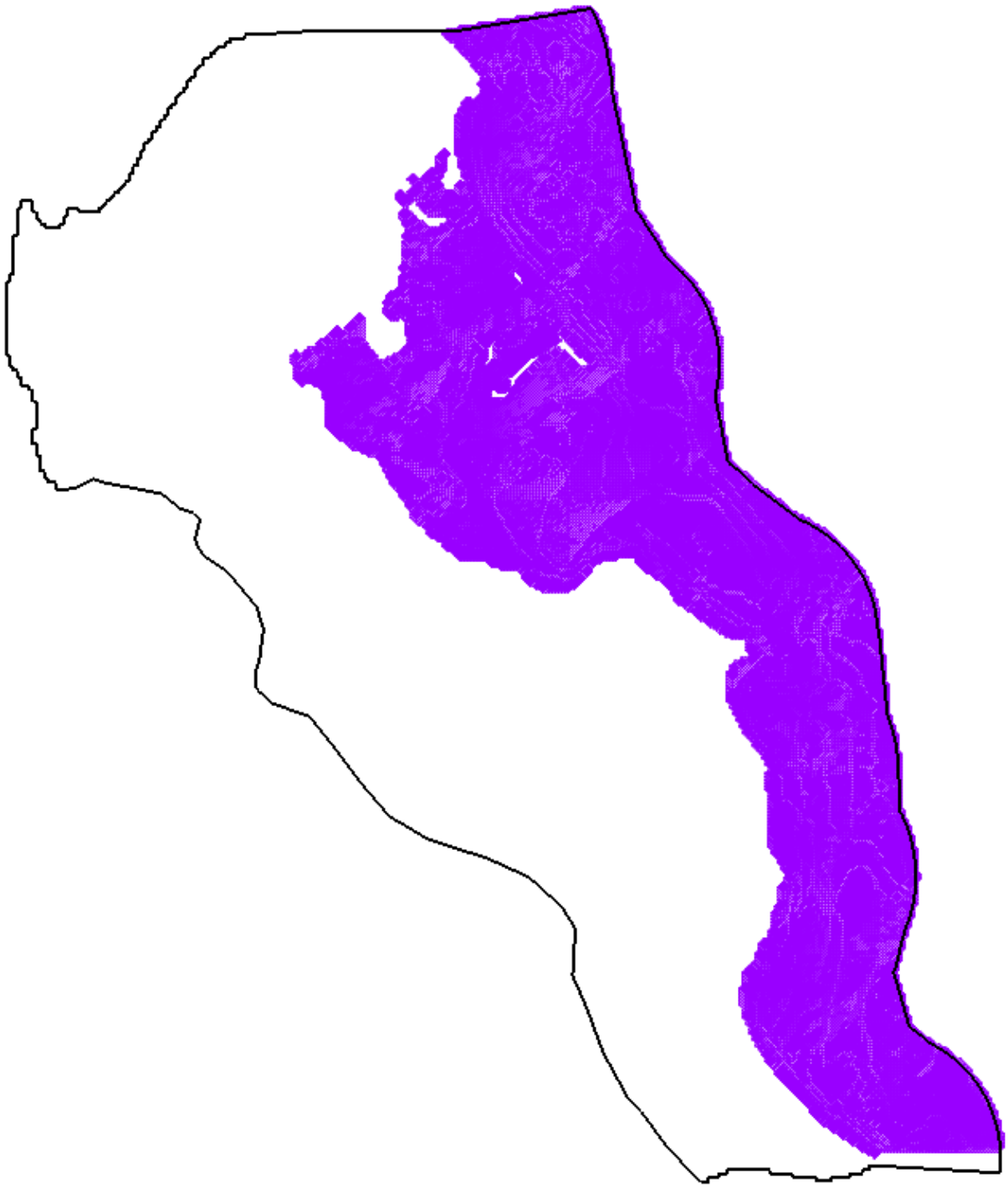

Figure S10: Location of model cells with CHD boundary condition.

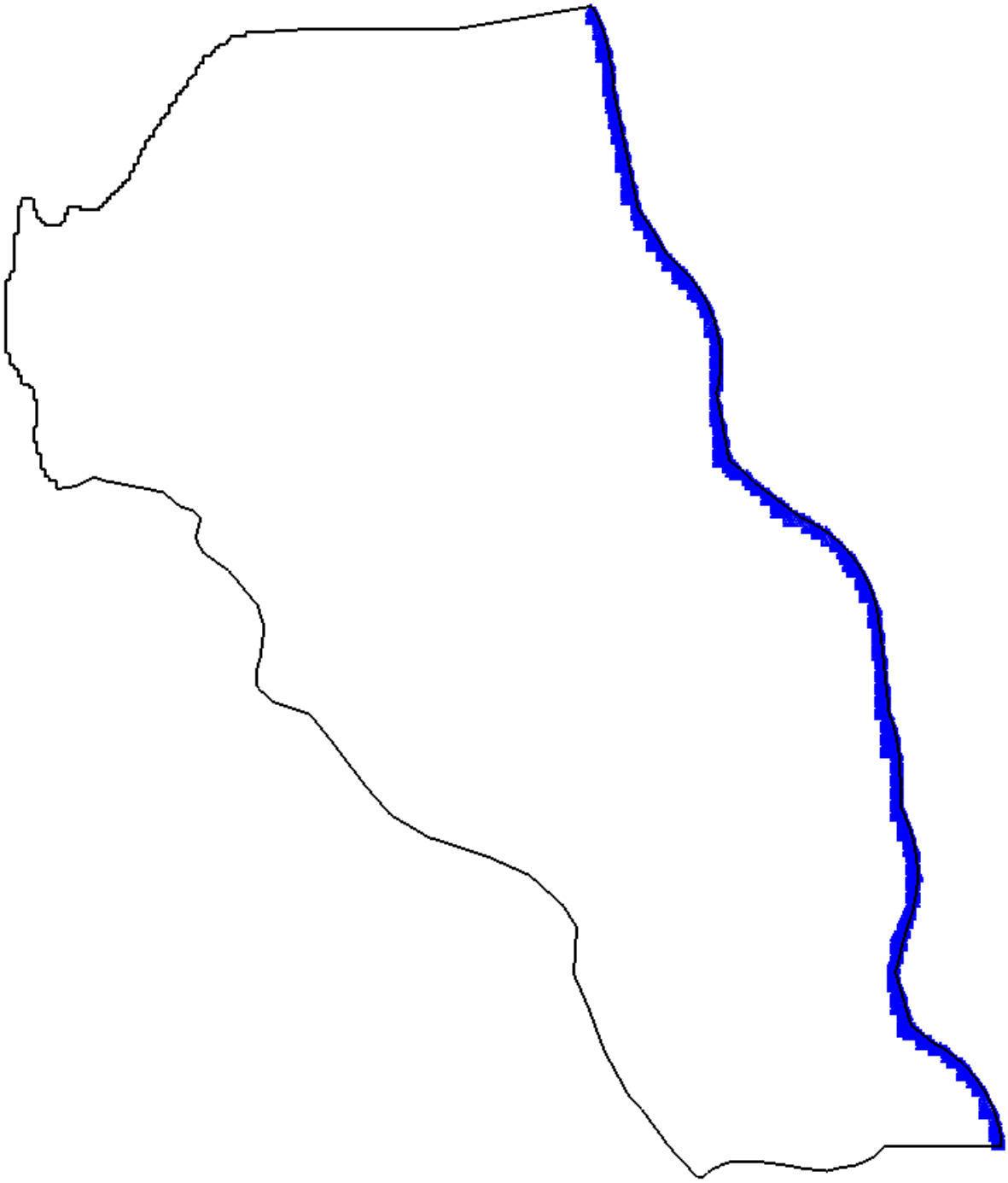

Figure S11: Location of model cells with CNC boundary condition.